NATIONAL ADVISORY COMMITTEE FOR AERONAUTICS

TECHNICAL NOTE

No. 1504

SIDESLIP ANGLES AND VERTICAL-TAIL LOADS DEVELOPED BY PERIODIC CONTROL DEFLECTIONS

By Harvard Lomax

Ames Aeronautical Laboratory
Moffett Field, Calif.

Washington
January 1948

NATIONAL ADVISORY COMMITTEE FOR AERONAUTICS

TECHNICAL NOTE NO. 1504

SIDESLIP ANGLES AND VERTICAL-TAIL LOADS DEVELOPED BY PERIODIC CONTROL DEFLECTIONS

By Harvard Lomax

SUMMARY

Dynamic maneuvers consisting of periodic rudder and aileron control deflections are considered with respect to the maximum sideslip angles developed and the position of the rudder at the time of maximum sideslip. The most logical and simplest maneuver of such a type is shown to be that in which the rudder is oscillating with the aileron locked. Such a maneuver is compared to two other dynamic maneuvers, the rudder kick and the rolling pull-out. The comparison shows that for certain configurations one and one-half cycles of rudder motion are sufficient to produce tail loads of the same order of magnitude as those obtained in a rolling pull-out maneuver; and that for all configurations one cycle of rudder motion is sufficient tc produce more sideslip than that obtained from the rudder kick.

A method is also given for computing the maximum sideslip angles when the forces and moments are nonlinear functions of the sideslip.

INTRODUCTION

The maneuvers analyzed in this report were those of an airplane in a side-slipping oscillation produced by certain combinations of periodic rudder and aileron control movements. Two principal types of these maneuvers were considered: one in which the airplane had reached a steady-state oscillation called the fishtailing maneuver; and the other in which the airplane was in the transient state preceding the steady-state oscillations.

Since the purpose of the report was to discover the maximum tail loads which would occur in the steady-state fishtailing and transient maneuvers, all principal types of control variations and combinations were considered. This was done by giving the rudder a periodic oscillation and superimposing the effects of the aileron

oscillations. In this manner three basic maneuvers were defined: maneuver A in which the ailerons were locked; maneuver B in which the ailerons were applied so as to hold the wings level; and maneuver C in which the ailerons were applied so as to reduce the roll. In order to assess the value of such maneuvers as criteria for critical tail loading, the maximum sideslip angles obtained from them were compared with the maximum sideslip angles obtained from two other dynamic maneuvers, the rudder kick and the rolling pull-out.

The analysis was carried out by means of the well-known lateral-stability equations(reference 1) in which for convenience the rudder and aileron motions were assumed to be sinusoidal functions of time. Numerical computations were made using a large number of derivatives representative of conventional airplane design to verify the general theory developed.

The results of the computations showed that, when in a state of resonance with the rudder, the motion of the airplane could be obtained with satisfactory accuracy from the solution of a much simpler equivalent differential equation of second degree. By means of this modification the analysis was extended to include the effects of nonlinear variations of the forces and moments with the angle of sideslip.

COEFFICIENTS AND SYMBOLS

The coefficients and symbols defined herein are referred to the so-called "stability axes," the origin of which is fixed at the center of gravity. At the beginning of the motion the Z-axis is in the plane of symmetry and perpendicular to the relative air stream, the X-axis is in the plane of symmetry and parallel to the relative air stream, and the Y-axis is perpendicular to the Z- and X-axes; and thenceforth throughout the motion of the airplane the axes remain fixed with respect to the airplane.

b	wing span, feet
S	wing area, square feet
m	mass of airplane, slugs
l	distance from center of gravity to rudder hinge line, feet
g	acceleration due to gravity, feet per second squared

k_X radius of gyration about X-axis, feet

k_Z radius of gyration about Z-axis, feet

i_a dimensionless radius of gyration about X-axis $\left[\left(\frac{2k_X}{b}\right)^2\right]$

i_c dimensionless radius of gyration about Z-axis $\left[\left(\frac{2k_Z}{b}\right)^2\right]$

ρ air density, slugs per cubic foot

V velocity of airplane along flight path, feet per second

q free-stream dynamic pressure $(\frac{1}{2}\rho V^2)$, pounds per square foot

β_a angle of sideslip, radians

β° angle of sideslip, degrees

p rate of roll, radians per second

$\hat{p}$ rate of roll with respect to aerodynamic time

r rate of yaw, radians per second

$\hat{r}$ rate of yaw with respect to aerodynamic time

v component of flight velocity along Y-axis, feet per second

φ angle of bank, radians

C_Y lateral-force coefficient $\left(\frac{\text{force along Y-axis}}{qS}\right)$

C_l rolling-moment coefficient $\left(\frac{\text{moment about X-axis}}{qSb}\right)$

ΔC_l increment in applied rolling-moment coefficient

C_n yawing-moment coefficient $\left(\frac{\text{moment about Z-axis}}{qSb}\right)$

ΔC_n increment in applied yawing-moment coefficient

t	time, seconds
τ	aerodynamic time $[t(\rho VS/m)]$
μ	relative density coefficient $(m/\rho Sb)$
δ_r	rudder angle (positive when trailing edge to the right), degrees
δ_a	aileron angle, degrees
δ_{a_1}, δ_{a_2}	maximum values of components of aileron motion
$C_{n\delta_a}$	rate of change of yawing-moment coefficient with aileron deflection $\left(\frac{\partial C_n}{\partial \delta_a}\right)$, per degree
$C_{n\delta_r}$	rate of change of yawing-moment coefficient with rudder deflection $\left(\frac{\partial C_n}{\partial \delta_r}\right)$, per degree
$C_{l\delta_a}$	rate of change of rolling-moment coefficient with aileron angle $\left(\frac{\partial C_l}{\partial \delta_a}\right)$, per degree
A	part of root of stability quartic, damping factor
A_1	damping factor, maneuver B
B	part of root of stability quartic, frequency factor
B_1	frequency factor, maneuver B
C_{Y_β}	$\left(\frac{\partial C_Y}{\partial \beta}\right)$
C_{l_β}	$\left(\frac{\partial C_l}{\partial \beta}\right)$
C_{n_β}	$\left(\frac{\partial C_n}{\partial \beta}\right)$

C_{l_r} $\left[\frac{\partial C_l}{\partial\left(\frac{rb}{2V}\right)}\right]$

C_{n_r} $\left[\frac{\partial C_n}{\partial\left(\frac{rb}{2V}\right)}\right]$

C_{l_p} $\left[\frac{\partial C_l}{\partial\left(\frac{pb}{2V}\right)}\right]$

C_{n_p} $\left[\frac{\partial C_n}{\partial\left(\frac{pb}{2V}\right)}\right]$

$l_{1,2,3}$ coefficients of β_1, β_2, and β_3 in nonlinear expression for C_Y

$M_{1,2,3}$ coefficients of β_1, β_2, and β_3 in nonlinear expression for C_n

l_p $\left(\frac{C_{l_p}}{i_a}\right)$

l_β $2\mu\left(\frac{C_{l_\beta}}{i_a}\right)$

k aileron yaw factor $\left(\frac{C_{n_{\delta_a}}}{C_{l_{\delta_a}}}\right)$

Q ratio of maximum rolling velocity developed in maneuver C to that developed in maneuver A

α frequency of sideslip oscillation in nonlinear solution

ω	frequency of rudder oscillation, 2 π times cycles per unit aerodynamic time
N	number of half cycles
H_1, H_2	components of sideslip produced by sinusoidal rolling moment

Subscripts

r, a – rudder, aileron

o	maximum value of amplitude
R	maximum value of amplitude at resonance
u	refers to solution for unit control deflection
l	refers to motion produced by rolling moment only
n	refers to motion produced by yawing moment only
ail yaw	refers to yawing moment due to aileron deflection
RK	refers to rudder kick
RP	refers to rolling pull-out
N	refers to number of half-cycles
A	refers to maneuver A, ailerons locked
B	refers to maneuver B, ailerons applied to maintain zero rolling velocity
C	refers to maneuver C, ailerons applied to reduce rolling velocity

FISHTAILING MANEUVER

Analysis

For all maneuvers considered the analysis was initiated by solving the well-known lateral stability equations

$$\frac{d\hat{p}}{d\tau} = \hat{p}\frac{Cl_p}{i_a} + \hat{r}\frac{Cl_r}{i_a} + 2\mu\beta\frac{Cl_\beta}{i_a} + \Delta Cl\frac{2\mu}{i_a}$$

$$\frac{d\hat{r}}{d\tau} = \hat{p}\frac{Cn_p}{i_c} + \hat{r}\frac{Cn_r}{i_c} + 2\mu\beta\frac{Cn_\beta}{i_c} + \Delta Cn\frac{2\mu}{i_c} \qquad (1)$$

$$\frac{d\beta}{d\tau} = \tfrac{1}{2}C_L\varphi - \hat{r} + \beta\tfrac{1}{2}C_{Y_\beta}$$

for the initial conditions $\hat{p} = \hat{r} = \beta = \varphi = 0$ at $\tau = 0$. Since the equations are linear, their solutions are obtained by standard methods from the use of operators. (See, e.g., reference 2.)

Maneuver A: Ailerons locked.— The particular solution for the rate of change of sideslip produced by holding the aileron fixed $\Delta Cl = 0$ and suddenly deflecting the rudder by an amount δ_r can be written

$$\left(\frac{d\beta}{d\tau}\right)_u \left(\frac{i_c}{2\,\delta_r Cn_{\delta_r}\mu}\right) = C_1e^{\lambda_1\tau} + C_2e^{\lambda_2\tau} + (C_3\cos B\tau + C_4\sin B\tau)e^{A\tau} \qquad (2)$$

where the constants λ_1, λ_2, A, B, C_1, C_2, C_3, and C_4 depend upon the stability derivatives of equation (1). These constants are presented in table II for each of the 27 different combinations of derivatives listed in table I. The maximum value of sideslip in an aileron-locked rudder-oscillating maneuver can be determined by the use of these derivatives in conjunction with equation (2). However, the complexity of the results obtained from the use of equation (2) led to a search for some simplifying assumptions which would still give reasonable accuracy. Such a simplified

solution would be especially desirable for use in the study of nonlinear aerodynamic characteristics and in the study of maneuvers in which the aileron was applied. It would also provide a simple closed formula for the maximum sideslip which would be useful in interpolating for derivatives not listed in the table. An inspection of table II immediately suggests that the terms containing C_1, C_2, and C_3 be neglected in comparison with the term C_4. A column of $1/B$ is given in table III and a comparison of this quantity with C_4 also suggests that the equation $C_4 = -1/B$ will hold. Finally then equation (2) is reduced to

$$\left(\frac{d\beta}{d\tau}\right)_u = -\frac{2\delta_r C_{n_{\delta_r}} \mu}{i_c B} e^{A\tau} \sin B\tau \tag{3}$$

The check on the accuracy of results derived by the use of equation (3) rather than equation (2) was provided by solving for the maximum steady-state sideslip using both equations and comparing the results. This comparison which will be presented later showed that the use of equation (3) was justified for practical results.

Equation (3) gives the rate of change of sideslip for a so-called "unit" deflection of the rudder. This is very useful, since from it the sideslip from any rudder deflection $\delta_r(\tau)$ can be built up by suitable superposition (reference 2). Thus

$$\beta = \int_0^\tau \left[\frac{d\beta(x)}{dx}\right]_u \delta_r(\tau - x)\,dx \tag{4}$$

where x is a dummy variable of integration.

The discussion in this report will be limited to oscillations produced by a sinusoidal control-surface variation given by the equation $\delta_r(\tau) = \delta_{r_0} \sin \omega\tau$. The choice of such a control variation was brought about obviously by convenience. If, however, some other periodic control motion is chosen, the resulting airplane motion brought about by its application can be found by a suitable superposition of the sinusoidal results. The type of superposition

is given by expanding the new function in terms of a Fourier series. Further, the expansion can always be made in a series containing only sine terms if the function is periodic and zero at time zero.

For the limiting case in which the control motion is chosen to be the so-called "square wave" the expansion is well known as

$$\delta_r = \delta_{r_o} \frac{4}{\pi} \sum_{n=1}^{\infty} \frac{1}{2n-1} \sin \omega (2n-1) \tau \qquad (5)$$

It can be shown that the contribution to the maximum sideslip of the third harmonic is at most less than one-tenth of the contribution of the first harmonic, so that in the summation the contribution of the third harmonic is one-thirtieth of that of the first harmonic. Thus the only important effect of using a square wave as given by equation (5) rather than a pure sine wave of the same frequency is to increase the maximum amplitude of the sideslip computed for the sinusoidal control by the factor $4/\pi$. This results in an increase of about 27 percent in maximum sideslip for the square wave over the sine wave.

Use of the square wave would, of course, be unduly conservative, since it represents an unattainable upper limit. The choice of any other periodic function is purely a matter of judgment. It is believed, however, that the sine wave is not unconservative but rather a fair average of what the pilot is likely to apply.

To obtain the maximum sideslip from a sinusoidal rudder control, then, such that

$$\delta_r(\tau) = \delta_{r_o} \sin \omega\tau$$

equation (4) reduces to

$$\beta_A = \frac{-2\delta_{r_o} C_{n\delta_r} \mu}{i_c B} \int_o^{\tau} e^{Ax} \sin Bx \sin \omega(\tau - x) dx \qquad (6)$$

The solution to equation (6) is

$$\beta = \frac{-\delta_{r_o} C_{n_{\delta_r}} \mu}{i_c B} \left\{ \left[G_1 \cos B\tau + (G_2 + G_3) \sin B\tau \right] e^{A\pi} \right.$$

$$\left. - G_1 \cos \omega\tau - (G_3 - G_2) \sin \omega\tau \right\} \tag{7}$$

where

$$\left.\begin{aligned} G_1 &= \frac{A}{A^2 + (\omega+B)^2} - \frac{A}{A^2 + (\omega-B)^2} \\ G_2 &= \frac{\omega + B}{A^2 + (\omega+B)^2} \\ G_3 &= \frac{\omega - B}{A^2 + (\omega-B)^2} \end{aligned}\right\} \tag{8}$$

The steady-state solution of equation (7) can be put in the form

$$\beta_A = \frac{-\delta_{r_o} C_{n_{\delta_r}} \mu}{A\, B\, i_c} \left[\frac{2\left(\frac{A}{B}\right)}{\sqrt{\left\{ \left(\frac{A}{B}\right)^2 + \left[1 - \left(\frac{\omega}{B}\right)\right]^2 \right\}\left\{ \left(\frac{A}{B}\right)^2 + \left[1 + \left(\frac{\omega}{B}\right)\right]^2 \right\}}} \right]$$

$$\times \sin\ (\omega\tau + \gamma) \tag{9}$$

where

$$\gamma = \arctan \frac{2\left(\frac{\omega}{B}\right)\left(\frac{A}{B}\right)}{\left(\frac{A}{B}\right)^2 + 1 - \left(\frac{\omega}{B}\right)^2} \tag{10}$$

Equation (10) is more useful, however, when it is used to express the ratio of the rudder angle when the airplane is at its maximum sideslip angle to the maximum rudder angle. This expression is

$$\frac{(\delta_r)_{\beta=\beta A_O}}{\delta_{r_O}} = \cos\gamma = \frac{\left(\frac{A}{B}\right)^2 + 1 - \left(\frac{\omega}{B}\right)^2}{\sqrt{\left(2\frac{\omega}{B}\frac{A}{B}\right)^2 + \left[\left(\frac{A}{B}\right)^2 + 1 - \left(\frac{\omega}{B}\right)^2\right]^2}} \tag{11}$$

Equations (9) and (11) are the complete solution for the aileron-locked maneuver for any ratio of the applied rudder frequency to the natural frequency of the airplane ω/B and for any ratio of natural damping to natural airplane frequency A/B. Principal interest, of course, is centered on the special case of these solutions when the rudder motion and the airplane motion are in resonance. This resonant value can be determined by finding the maximum value of β in equation (9).

This maximum occurs when $\frac{\omega}{B} = \sqrt{1 - \left(\frac{A}{B}\right)^2}$ and for such a value

equations (9) and (11) reduce, respectively, to

$$\beta_{A_R} = \frac{\delta r_o \, Cn_{\delta_r} \mu}{ABi_c} \tag{12}$$

and

$$\frac{(\delta_r)_{\beta=\beta_{A_R}}}{\delta r_o} = -\frac{A}{B} \tag{13}$$

Maneuver B: Ailerons applied to hold wings level.- An analysis of this maneuver was considered to some extent in reference 3, but no consideration was given to the effects of aileron yawing moment or to the effects of dihedral. These effects are of varying importance, depending on the magnitude of the dihedral and directional stability. The procedure used in this section was to develop the equations for sideslip and rudder position, first considering the effect of dihedral and neglecting that of the aileron yawing moment. The development was next extended to include the effect of the aileron yawing moment.

Effect of dihedral.- Since the rate of roll and angle of bank are being held constant at zero, equation (1) reduces to

$$\left.\begin{aligned} 0 &= \hat{r}\,\frac{Cl_r}{i_a} + 2\mu\beta\,\frac{Cl_\beta}{i_a} + \Delta Cl\,\frac{2\mu}{i_a} \\ \frac{d\hat{r}}{d\tau} &= \hat{r}\,\frac{Cn_r}{i_c} + 2\mu\beta\,\frac{Cn_\beta}{i_c} + \Delta Cn\,\frac{2\mu}{i_c} \\ \frac{d\beta}{d\tau} &= -\hat{r} + \tfrac{1}{2}\,\beta CY_\beta \end{aligned}\right\} \tag{14}$$

In order to simplify the analysis the term $\hat{f}\frac{C_{l_r}}{i_a}$ which is small as compared with $2\mu\beta\frac{C_{l_\beta}}{i_a}$ was neglected and line 1 of equation (14) was written

$$\delta_a C_{l_{\delta_a}} = -\beta C_{l_\beta} \tag{15}$$

Later, some computations were made including the term C_{l_r} so that some idea of the magnitude of its effect could be obtained. These results are presented in the section headed Discussion.

The remaining terms of equation (14) can be rearranged to form a second-order differential equation in β, thus,

$$\frac{d^2\beta}{d\tau^2} - \left(\frac{C_{n_r}}{i_c} + \frac{1}{2}C_{Y_\beta}\right)\frac{d\beta}{d\tau} + \left(\frac{1}{2}C_{Y_\beta}\frac{C_{n_r}}{i_c} + \frac{2\mu C_{n_\beta}}{i_c}\right)\beta$$

$$+ \frac{2\delta_{r_o}C_{n_{\delta_r}}\mu}{i_c}\sin\omega\tau = 0 \tag{16}$$

where the yawing moment due to sinusoidal rudder displacement $\delta_{r_o} C_{n_{\delta_r}} \sin\omega\tau$ has been substituted for ΔC_n. Equation (16) can be solved by ordinary methods to yield a resonant solution

$$\beta_B = \frac{\delta_{r_o}C_{n_{\delta_r}}\mu}{A_1 B_1 i_c}\sin\left(\tau\sqrt{B_1^2 - A_1^2} + \tan^{-1}\frac{\sqrt{B_1^2 - A_1^2}}{A_1}\right) \tag{17}$$

The expressions corresponding to equations (12) and (13) for this case are

$$\beta_{B_R} = \frac{\delta_{r_o} C_{n\delta_r} \mu}{A_1 B_1 i_c} \tag{18}$$

and

$$\frac{(\delta_r)_{\beta=\beta_{B_R}}}{\delta_{r_o}} = -\frac{A_1}{B_1} \tag{19}$$

where

$$\left.\begin{aligned} A_1 &= \tfrac{1}{2}\left(\frac{C_{n_r}}{i_c} + \tfrac{1}{2} C_{Y_\beta}\right) \\ B_1 &= \sqrt{-\tfrac{1}{4}\left(\frac{C_{n_r}}{i_c} - \tfrac{1}{2} C_{Y_\beta}\right)^2 + \frac{2 C_{n_\beta} \mu}{i_c}} \end{aligned}\right\} \tag{20}$$

But since $\frac{C_{n_r}}{i_c}$ and $\frac{1}{2} C_{Y_\beta}$ are small, one-fourth the square of their difference is negligible as compared to $2\mu \frac{C_{n_\beta}}{i_c}$, hence,

$$B_1 \approx \sqrt{2\mu \frac{C_{n_\beta}}{i_c}} \tag{21}$$

Effect of aileron yawing moment.- Equation (18) gives the maximum resonant sideslip developed with ailerons applied so as to hold wings level, provided the ailerons produce no yawing moment. The effect of aileron yawing moment can be estimated closely enough by considering equation (15) with (16) and using a solution to equation (16) which is not quite the resonant solution given by equation (17), but rather the simpler solution

$$\beta_B = \frac{\delta_{r_o} C_{n_{\delta_r}} \mu}{A_1 B_1 i_c} \cos B_1 \tau \tag{22}$$

where $\frac{1}{2} C_{Y_\beta} \frac{C_{n_r}}{i_c}$ is neglected when added to $2\mu \frac{C_{n_\beta}}{i_c}$, so that B_1 is again given by equation (21). A comparison of equation (22) with equation (17) shows that the difference between the two equations is manifest in a slight phase shift of magnitude $\left(\frac{\pi}{2} + \tan^{-1} \sqrt{\frac{B_1^2 - A_1^2}{A_1}}\right) \frac{1}{B_1}$. At a time when the value of the sideslip given by equation (17) is a maximum, this phase shift causes the value given by equation (22) to be less by a factor

$$\sqrt{\frac{2\mu \frac{C_{n_\beta}}{i_c} - \frac{1}{4}\left(\frac{C_{n_r}}{i_c} - \frac{1}{2} C_{Y_\beta}\right)^2}{2\mu \frac{C_{n_\beta}}{i_c} + \frac{1}{2} C_{Y_\beta} \frac{C_{n_r}}{i_c}}}$$

Using the values of the derivatives from table I in the preceding expression shows the correction brought about by its use is small enough to be neglected in estimating the effects of the aileron yawing moment. Accordingly, the simpler expression for sideslip given by equation (22) will be used in the remainder of this section. Let the aileron control movement be given by

$$\delta_a = \delta_{a_1} \sin B_1 \tau + \delta_{a_2} \cos B_1 \tau \tag{23}$$

so that the corresponding moment equations will be

$$\left.\begin{aligned} \Delta C_l &= \delta_{a_1} C_{l_{\delta_a}} \sin B_1 \tau + \delta_{a_2} C_{l_{\delta_a}} \cos B_1 \tau \\ \Delta C_n &= k\delta_{a_1} C_{l_{\delta_a}} \sin B_1 \tau + k\delta_{a_2} C_{l_{\delta_a}} \cos B_1 \tau \end{aligned}\right\} \tag{24}$$

where k is the aileron yaw factor

$$k = C_{n_{\delta_a}} / C_{l_{\delta_a}} \tag{25}$$

Adding to equation (24) the effect of the rudder gives for ΔC_n

$$\Delta C_n = (\delta_{r_o} C_{n_{\delta_r}} + k\delta_{a_1} C_{l_{\delta_a}}) \sin B_1 \tau + k\delta_{a_2} C_{l_{\delta_a}} \cos B_1 \tau \tag{26}$$

Substituting for $\delta_{r_o} C_{n_{\delta_r}} \sin \omega\tau$ in equation (16) the disturbance indicated by equation (26) the expression corresponding to equation (22) becomes:

$$\beta_B = \frac{\mu}{A_1 B_1 i_c} \left[(\delta_{r_o} C_{n_{\delta_r}} + k\delta_{a_1} C_{l_{\delta_a}}) \cos B_1\tau - k\delta_{a_2} C_{l_{\delta_a}} \sin B_1\tau \right] \tag{27}$$

Placing this in equation (15) yields the two equations

$$\delta_{a_1} C_{l_{\delta_a}} = \frac{C_{l_\beta} \mu}{A_1 B_1 i_c} k\delta_{a_2} C_{l_{\delta_a}}$$

$$\delta_{a_2} C_{l_{\delta_a}} = -\frac{\mu C_{l_\beta}}{A_1 B_1 i_c} (\delta_{r_o} C_{n_{\delta_r}} + k\delta_{a_1} C_{l_{\delta_a}})$$

These can be solved for δ_{a_1} and δ_{a_2}. Using equations (27) and (18) the ratio of $(\beta_{B_R})_{\text{ail yaw}}$, the maximum sideslip developed with aileron yaw considered, to β_{B_R}, the maximum sideslip developed neglecting aileron yaw is

$$\frac{(\beta_{B_R})_{\text{ail yaw}}}{\beta_{B_R}} = \frac{1}{\sqrt{1 + \left(\frac{k\mu C_{l_\beta}}{A_1 B_1 i_c}\right)^2}} \tag{28}$$

Maneuver C: Ailerons applied so as to reduce the roll.- The magnitude of the sideslip developed in this maneuver depends upon the amount the roll is reduced by the ailerons and the phase difference between the aileron and rudder movements. Certainly the most critical phase relationship should be considered, since for such short time intervals the pilot would not be expected to hold any fixed phase relationship between the ailerons and the rudder. However, the amount the roll is reduced is a somewhat arbitrary matter and consequently the factor Q, the ratio of the maximum rolling velocity developed in this maneuver to that developed in an aileron-locked maneuver, will be a parameter in the solutions.

The analysis will be restricted to the case in which the aileron and rudder control movements have the same period. In the study of maneuver B this was not an assumption but a necessary condition for maintaining wings level. In addition the assumptions will be made as before that C_{l_r} can be neglected, and again the solution to equation (1) for the sinusoidal rudder deflection corresponding to equation (22), will be used in which the sideslip is 90° out of phase with the yawing moment at resonance.

Again consider that the aileron control motion and the corresponding moments be given by equations (23) and (24). The steady-state solution of equation (1) for the sideslip caused by the rolling moment of equation (24) is given by the equation

$$\beta_l = C_{l_{\delta_a}} \frac{2\mu}{i_a} \left[(\delta_{a_1} H_2 - \delta_{a_2} H_1) \sin B\tau + (\delta_{a_1} H_1 + \delta_{a_2} H_2) \cos B\tau \right] \tag{29}$$

where the values of H_1 and H_2 were determined by a complete numerical solution of equation (1) in which nothing was neglected. These values are presented in table III for each of the 27 configurations of table I. The rolling velocity caused by the rolling moment is determined by using equations (24) and (29) in equation (1) and neglecting C_{l_r} thus:

$$\hat{p}_l = \left(\frac{B\delta_{a_2}^* - l_p\delta_{a_1}^*}{l_p^2 + B^2} \right) \frac{2\mu C_{l\delta_a}}{i_a} \sin B\tau$$

$$- \left(\frac{B\delta_{a_1}^* + l_p\delta_{a_2}^*}{l_p^2 + B^2} \right) \frac{2\mu C_{l\delta_a}}{i_a} \cos B\tau \qquad (30)$$

where

$$\left.\begin{aligned} \delta_{a_2}^* &= \delta_{a_2} + l_\beta H_2\delta_{a_2} + l_\beta H_1\delta_{a_1} \\ \delta_{a_1}^* &= \delta_{a_1} + l_\beta H_2\delta_{a_1} - l_\beta H_1\delta_{a_2} \end{aligned}\right\} \qquad (31)$$

If the rudder disturbance is

$$\delta_r = \delta_{r_o} \sin B\tau \qquad (32)$$

so that the total yawing moment is given again by equation (26), then the sideslip and rolling velocity will be, respectively,

$$\beta_n = -\left(\beta_{A_R} + \frac{k\delta_{a_1} C_{l\delta_a}\mu}{AB\, i_c} \right) \cos B\tau + \frac{k\delta_{a_2} C_{l\delta_a}\mu}{AB\, i_c} \sin B\tau \qquad (33)$$

and

$$\hat{p}_n = \left[\frac{-B\beta A_R l_\beta - \dfrac{k l_\beta C_{l_{\delta_a}} \mu}{AB\, i_c} (B\delta_{a_1} + l_p \delta_{a_2})}{l_p^2 + B^2} \right] \sin B\tau$$

$$+ \left[\frac{l_p \beta A_R l_\beta + \dfrac{k l_\beta C_{l_{\delta_a}} \mu}{AB\, i_c} (l_p \delta_{a_1} - B\delta_{a_2})}{l_p^2 + B^2} \right] \cos B\tau \qquad (34)$$

Equations (30) and (34) can now be added to give the total rolling velocity for the applied control movement given by equations (23) and (32). The restriction applied to the maneuver is that the maximum value of this total rolling velocity should be Q times the maximum value of the rolling velocity for the same rudder movement but with the ailerons fixed. This condition leads to the equation

$$\left[\frac{\delta_{a_1} C_{l_{\delta_a}}}{\beta A_R} - \frac{l_\beta C_{l_\beta} \left(H_1 - \dfrac{k\, i_a}{2 i_c AB} \right)}{(1 + H_2 l_\beta)^2 + \left(H_1 l_\beta - \dfrac{k i_a l_\beta}{2 i_c AB} \right)^2} \right]^2$$

$$+ \left[\frac{\delta_{a_2} C_{l_{\delta_a}}}{\beta A_R} - \frac{C_{l_\beta} (1 + H_2 l_\beta)}{(1 + H_2 l_\beta)^2 + \left(H_1 l_\beta - \dfrac{k i_a l_\beta}{2 i_c AB} \right)^2} \right]^2$$

$$= \frac{Q^2 C_{l_\beta}{}^2}{(1 + H_2 l_\beta)^2 + \left(H_1 l_\beta - \dfrac{k i_a\, l_\beta}{2 i_c AB} \right)^2} \qquad (35)$$

which gives the relationship between δ_{a_1} and δ_{a_2}, which must be satisfied for any particular configuration and choice of Q. Equation (35) is the equation of a circle in terms of $\frac{\delta_{a_1} C_{l_{\delta_a}}}{\beta_{A_R}}$ and $\frac{\delta_{a_2} C_{l_{\delta_a}}}{\beta_{A_R}}$ of radius

$$-C_{l_\beta} Q \sqrt{\frac{1}{(1+H_2 l_\beta)^2 + \left(H_1 l_\beta - \frac{k i_a l_\beta}{2 i_c AB} \right)^2}}$$

Points on this circle represent the different phase relationships which the aileron may take relative to the rudder always maintaining the same value of maximum rolling velocity. As $\frac{\delta_{a_1} C_{l_{\delta_a}}}{\beta_{A_R}}$ and $\frac{\delta_{a_2} C_{l_{\delta_a}}}{\beta_{A_R}}$ move around this circle the amplitude of the sideslip has both a maximum and a minimum. If Q is set equal to one, the circle must always pass through the origin of the coordinate system as this special point, where $\delta_{a_1} = \delta_{a_2} = 0$, represents the aileron-locked maneuver. On the other hand, when Q is set equal to zero the circle reduces to a point and this point represents maneuver B.

In order to find the point where the maximum resonant amplitude of the sideslip β_{C_R} is obtained, the sum of equations (29) and (33) must be considered. Thus,

$$\left(\frac{\beta_c}{\beta_{AR}}\right)^2 = \left[\frac{2\delta_{a_1} C_{l_{\delta_a}} \mu H_2}{i_a \beta_{AR}} - \frac{2\delta_{a_2} C_{l_{\delta_a}} \mu}{i_a \beta_{AR}}\left(H_1 - \frac{k\, i_a}{2 i_c AB}\right)\right]^2$$

$$\left[\frac{2\delta_{a_2} C_{l_{\delta_a}} \mu H_2}{i_a \beta_{AR}} - 1 + \frac{2\delta_{a_1} C_{l_{\delta_a}} \mu}{i_a \beta_{AR}}\left(H_1 - \frac{k\, i_a}{2 i_c AB}\right)\right]^2 \quad (36)$$

Equations (35) and (36) are sufficient to fix $\frac{\beta C_R}{\beta_{AR}}$ for any configuration and value of Q.

Discussion

Maneuver A: Ailerons locked.- Since the equations developed from the analysis of maneuver A proved to be the most useful and important, they were most thoroughly studied both from a mathematical and a physical standpoint. Equation (12) summarizes the results for this maneuver in that it presents the maximum resonant value of sideslip. The fundamental check on this equation was to compare the maximum sideslip obtained by its use with the maximum sideslip obtained by the use of complete numerical solutions computed using all of equation (2). The results of this check are presented in table IV where the ratio of β_{A_R} as determined from the complete numerical solutions to the value of β_{A_R} as determined from equation (12) is tabulated for each of the 27 configurations under the heading $(\beta_{A_R})_{true}/(\beta_{A_R})_{approx}$. This ratio was also plotted in figure 1 against $C_{n_\beta o}$ with $C_{l_\beta o}$, as a parameter. The figure shows that for the entire range of configurations chosen, the error in using equation (12) was nowhere greater than 7 percent and this error occurred for the combination of low directional stability and high dihedral and, further, was conservative.

Data were obtained in level flight in the cruising condition at an average indicated airspeed of 245 miles per hour at a pressure altitude of 7500 feet. A total of 23 satisfactory runs were made with a range of periods from 1.45 to 3.2 seconds.

Values of the natural damping factor A and the natural frequency factor B were determined from damped-oscillation flight tests. A value of $C_{n_{\delta_r}}$ was determined from wind-tunnel tests of a powered 0.17-scale model and was verified by flight tests. These values were used in equation (12) to compute a value of β_{A_R}/δ_{r_o} of 3.15. The actual ratio of β_{A_R}/δ_{r_o} measured in the oscillating rudder flight tests was 3.02. Thus the maximum resonant sideslip predicted from equation (12) was within 5 percent of that obtained from flight tests and, further, was conservative. A further check on the theory was obtained by dividing the maximum value of sideslip angle obtained from a given rudder frequency by that obtained in resonance and comparing such values obtained from the flight test with those obtained by the use of equation (9). This comparison is shown in figure 5 for the range of rudder frequencies tested. The figure shows that excellent agreement was obtained between the theoretical values and those obtained from experiment. Similar agreement was obtained between flight tests and theory of the ratio of the rudder angle at maximum sideslip angle to the maximum rudder angle. (See fig. 6.)

Maneuver B: Ailerons applied to hold wings level.- In order to form some basis for the evaluation of maneuver B, equation (18) which was derived neglecting aileron yawing moment will be compared with equation (12) which gives the maximum sideslip for maneuver A. The ratio of the two sideslips is therefore

$$\frac{\beta_{B_R}}{\beta_{A_R}} = \frac{AB}{A_1B_1} \tag{37}$$

This ratio is given in table IV for the 27 configurations of table I, but the results can be summarized in figure 7 which is a plot of the equation (37) for configurations 1 through 6. This figure shows that for the values of $C_{l_\beta o}$ more negative than -0.0002, corresponding to values of effective dihedral greater than about 1°, maneuver A is more critical than maneuver B, and that this is independent of the value of directional stability.

An idea of how critical the resonant value of sideslip is with the ratio of the rudder period to the natural period of the airplane can be obtained from figures 2 and 3 in which equations (9) and (11) are plotted for a value of τ which makes equation (9) a maximum. These figures indicate that airplanes with relatively low values of A/B are less likely to attain the value of β_{AR} predicted by equation (12) since to do so the period of each rudder oscillation must be made relatively much closer to the natural period of the airplane. The likelihood of a pilot maintaining the period of a rudder oscillation within a given percentage of some fixed period is of course controversial. Analysis can only predict the value of sideslip obtained from any rudder frequency which the pilot might apply, and the limits of allowable rudder frequency which he must hold in order to maintain sensibly the resonant value of sideslip given by equation (12). In this latter connection, since it is maximum tail load rather than maximum sideslip which forms the basis of this report, figure 4 should be studied in conjunction with figure 3. To a first approximation the rudder angle can be multiplied by the rudder effectiveness factor $(\partial\alpha_t/\partial\delta_r)_{C_L}$ and added to the sideslip to form an effective sideslip angle on which tail loads can be based. Such a procedure indicated that the critical tail load can be higher than that obtained at resonance and that the critical range of frequencies can be extended somewhat. These differences, although small, can be computed readily for a particular tail-rudder combination once the resonant value of sideslip is known by the use of figures 2 and 3.

One last important effect of the aileron-locked maneuver can be seen by a study of equation (9). This equation shows that in a resonant maneuver at the time of maximum sideslip the rudder is in such a position as to increase the tail load. The ratio of this rudder angle to the maximum rudder angle is plotted in figure 4.

Experimental verification of the theoretical results predicted for maneuver A was obtained from flight tests of a conventional carrier-based airplane conducted by the flight research section at Ames. The flight-test data were obtained from an airplane, the rudder of which was connected to a rudder-oscillating mechanism operated by a direct-current motor and gear box. The pilot was furnished with an off-on switch, a rheostat for speed control, and indicating tachometer attached to the motor. The system gave very nearly sinusoidal rudder motions over a frequency range of about 20 to 70 cycles per minute and a rudder amplitude of about $\pm 1.2^\circ$.

The effects of aileron yaw are found by studying equation (28). The first thing to notice from this equation is that the sign of k is immaterial. That is, when C_{l_r} is neglected, the effects of adverse or favorable yawing moment are the same. Further, according to equation (28) the effects of aileron yaw must always decrease the maximum sideslip angle and such decrease will be more for high values of dihedral and less for high values of directional stability. These results are summarized in figure 8 where equation (28) is plotted against C_{l_β} for various values of k with values of the other necessary parameters as in configuration 5 of table I. This configuration was chosen as the worst case in that the ratio given by equation (28) would be the lowest.

The entire discussion of the effects of the aileron yaw is, of course, limited to the approximation made in equation (15), that $\frac{\hat{r}\, C_{l_r}}{i_a}$ was small enough to be neglected. As a check on this, some computations were made in which the term $\frac{\hat{r}\, C_{l_r}}{i_a}$ was included and the results of part of these computations are also plotted in figure 8. Only the results for a k of −0.06 are shown since they deviated most from the results already plotted. The figure shows that the maximum error occurs when $C_{l_\beta} = 0$ but that this error is less than 2 percent. This indicates that the conclusions of the preceding paragraph are not affected by considering C_{l_r} and that C_{l_r} can be neglected in the study of the effects of aileron yaw.

Maneuver C: Ailerons applied so as to reduce the roll.– Because of the complexity of the formulas developed in maneuver C, a numerical study was made for only a few cases. These cases were chosen to cover a wide enough range so that interpolation of the conclusions could be made. Thus the value of β_{C_R}/β_{A_R} given by equations (35) and(36) was determined and plotted against $C_{n_\beta o}$ for various values of Q and k for configurations 1, 3, and 5 of table I. The results are presented in figure (9) which gives the over-all picture of the fish-tailing maneuver.

These results have been derived by neglecting C_{l_r} and are only for a high value of $C_{l_\beta o}$ equal to −0.0021. The effects of C_{l_r} have been discussed in the analysis of maneuver B and the same conclusions are believed to apply to this maneuver. No variation of

H_1 and H_2 with C_{l_β} between $C_{l_\beta} = 0$ and -0.12 is given but the general effects of a reduced C_{l_β} can be estimated from figure 7. Thus, as the value of C_{l_β} approaches zero the curves of figure 9 would approach unity.

Figure 9 also shows that the effect of aileron yaw is not always to decrease the maximum sideslip angle. Thus the curves for $Q = 0$ (maneuver B) show a decrease in maximum sideslip angle due to aileron yaw, while the other curves show that aileron yaw may increase the maximum sideslip by as much as 5 percent for a value of $k = -0.025$. (This value of k corresponds to the approximate evaluation of aileron yawing moment $k = -\frac{C_L}{8}$.)

Considering the case of zero aileron yawing moment ($k = 0$), the curve in figure 9 for $Q = 1$ shows that the aileron-locked maneuver does not represent the case of maximum sideslip for the amount of roll developed, but that the ailerons can be applied so as to neither increase nor decrease the roll but so as to increase the sideslip by about 12 percent at a value of $C_{n_{\beta o}} = 0.0009$. A far more likely and important case, however, is that in which the pilot reduces the roll to some extent by use of the ailerons. The decrease in sideslip accompanying such a reduction in roll is linearly proportional to the reduction in roll. Thus since the curve for $Q = 0$, $k = 0$ (maneuver B with zero aileron yaw) represents the minimum sideslip coincident with zero roll, then if the roll is reduced 30 percent ($Q = 0.7$) from the maximum value obtainable at $Q = 1$, the sideslip will decrease by 30 percent of the difference between the curves for $Q = 1$ and $Q = 0$.

The figure shows that for high directional stability the sideslip developed for a value of $Q = 0.7$ is still only a few percent below the aileron-locked value and that even for $Q = 0.5$ the aileron-locked value is not ultraconservative. Therefore, since maneuver A is far easier to analyze than maneuver C and since the maximum sideslip angles developed in maneuver A are as critical as those developed in maneuver C for values of Q less than about 0.7, the maximum resonant sideslip developed in an aileron-locked maneuver given by equation (12) appears to be the most useful as a criterion for critical tail loads. Therefore only maneuver A is used in the comparison made with transient and other dynamic maneuvers in the remainder of the report.

TRANSIENT MANEUVERS

The limitation imposed by using only the steady-state results is serious and requires considerable discussion. In fact, the transient state which precedes the steady-state oscillation is of even greater practical importance because it represents a class of maneuvers far more common than the fishtailing maneuver. This class is any in which the rudder is used periodically but only for a few oscillations, the most common, of course, being one oscillation. Further, these maneuvers are performed by airplanes for which the fishtailing maneuver and other strenuous maneuvers such as the rolling pull-out have no practical importance.

The study of maneuver A in this transient state requires consideration of equation (7) for the effects of the exponentials with relatively small values of τ. Considering only the resonant case where $\omega \approx B$ and using the fact that at the points of maximum sideslip within a given half cycle the contribution to the sideslip of the terms containing G_2 and G_3 are negligible, and G_1 reduces to $-1/A$, the expression for β_A is obtained

$$\beta_A = \frac{-\delta_{r_o} C_{n_{\delta_r}} \mu}{AB\, i_c} \left(1 - e^{A\tau}\right) \cos B\tau$$

At the maximum values of β, $\tau = \frac{N\pi}{B}$ so that the ratio of the maximum sideslip after $N/2$ cycles β_{A_N} to the maximum sideslip in a steady state oscillation β_{A_R} is

$$\frac{\beta_{A_N}}{\beta_{A_R}} = \left(1 - e^{\frac{AN\pi}{B}}\right) \tag{38}$$

Equation (38) is plotted in figure 10 against N for various values of A/B. The results show that airplanes with a very low value of A/B require a large number of cycles to build up to their steady-state value but that airplanes with a value of A/B of around -0.3 develop 85 percent of their final amplitude in the first cycle. These results will be discussed at greater length in the next section.

COMPARISON OF MAXIMUM SIDESLIP DEVELOPED IN FISHTAILING AND TRANSIENT MANEUVERS WITH THAT DEVELOPED IN OTHER DYNAMIC MANEUVERS

The study of fishtailing and related maneuvers in connection with tail loads is of importance only if such maneuvers produce tail loads that are more critical than those of other reasonably probable maneuvers. There are two other dynamic maneuvers which have been advanced as a basis for critical loads and which will be used for comparison : the rudder kick and the rolling pull-out.

The first of these, the rudder kick, can be readily handled by the methods of this report by solving equation (6) for $\sin \omega (\tau - x) = 1$. If this is done and the maximum value of β is determined, the following value of sideslip results:

$$\beta_{RK} = -\delta_{r_o} \frac{2C_{n_{\delta_r}}\mu}{i_c B^2[(A/B)^2 + 1]} \left(e^{\frac{A\pi}{B}} + 1 \right)$$

But since the purpose of this section is to give an approximate comparison between the maximum sideslips developed, the assumption will be made throughout that $B^2 = C_{n_\beta} \frac{2\mu}{i_c}$ and that $(A/B)^2$ is negligible as compared to unity. This gives for the maximum sideslip in a rudder kick

$$\beta_{RK_o} = -\delta_{r_o} \frac{C_{n_{\delta_r}}}{C_{n_\beta}} \left(e^{\frac{A\pi}{B}} + 1 \right) \tag{39}$$

Making the same approximation in equation (12) and dividing the result by equation (39) yields the ratio of the maximum sideslip developed in an aileron-locked fishtailing maneuver β_{A_R} to the maximum sideslip developed in a rudder kick, β_{RK_o} as

$$\frac{\beta_{A_R}}{\beta_{RK_o}} \approx \frac{1}{2(A/B)\left(e^{\frac{A\pi}{B}} + 1\right)} \tag{40}$$

A plot of equation (40) against the ratio A/B is given in figure 11. The figure shows that the fishtailing maneuver is more critical than the rudder kick for values of A/B less than about −0.33. This difference is accentuated when considering critical tail loads by the fact that for the fishtailing maneuver at maximum sideslip the rudder is in a position to increase the tail load (equation (13)); whereas in a rudder kick at maximum sideslip the rudder is in a position to decrease the tail load.

The rolling pull-out has been analyzed to considerable extent in reference 4. For the purposes of comparison the simplified formula developed in that report will be used. This formula gave the maximum sideslip developed in a rolling pull-out β_{RP_o} as

$$\beta_{RP_o} = \tfrac{1}{2}\,\Delta C_l\,\frac{C_L}{C_{n_\beta}} \tag{41}$$

It would not be fair to compare equation (41) with (12) on the basis of equal lift coefficients since the rolling pull-out is an accelerated maneuver. However, if the two maneuvers are made at a fairly high speed and the rolling pull-out is made with a normal acceleration so as to increase the C_L of equation (41) to unity, a comparison between the two maneuvers is justifiable. Dividing equation (12) by equation (41) with $C_L = 1$, the following ratio is obtained:

$$\frac{\beta_{AR}}{\beta_{RP_o}} = \frac{\delta_{r_o} C_{n\delta_r}}{(A/B)\, \delta_a\, C_{l\delta_a}} \qquad (42)$$

Thus for the maneuvers to be equally severe, the maximum rudder angle needs only to be a fraction of the maximum aileron angle depending upon the value of $(C_{n\delta_r})\ /(C_{l\delta_a}\ A/B)$. Further, the position of the rudder in the rolling pull-out maneuver is neutral; whereas, as has been pointed out, in the fishtailing maneuver the rudder increases the load.

A somewhat better perspective of the relation between the rudder kick, the rolling pull-out and the maneuvers studied in this report can be obtained from a study of figure 12. Here the value of $\beta C_{n\beta}/\delta_{r_o} C_{n\delta_r}$ is plotted against A/B for the various maneuvers. The maneuvers previously discussed as transient maneuvers, where the airplane motion was still in a transient state or where only a few oscillations of the rudder were made, are represented by the solid lines. Corresponding values of N are the number of half cycles for which the rudder has been applied in order to reach the value of sideslip shown. The line for which N is equal to infinity is the steady-state fishtailing maneuver already discussed. For such a figure no restrictions on the value of A/B are necessary and the extension is made to the case of neutral stability where $A/B = 0$.

The shaded portion represents roughly the region of sideslips reached by the rolling pull-out (using a value of from 1/5 to 1/6 for the ratio $\delta_{r_o} C_{n\delta_r}/\delta_a C_{l\delta_a}$ and setting $C_L = 1$ in equation (41)). The figure shows that the fishtailing maneuver is less critical than the rolling pull-out for values of $-A/B > 0.2$, the two maneuvers are about equally critical for values of $-A/B$ between about 0.2 and 0.15, and the fishtailing maneuver is more critical for values of $-A/B$ less than about 0.15. If the rudder is oscillated for only one and a half cycles, however, the sideslip built up from such a maneuver is still greater than that in a rolling pull-out for values of $-A/B$ less than around 0.1.

The dotted curve of figure 12 represents the maximum sideslip developed by a rudder kick. The figure indicates that this value is less than that caused by one cycle of a rudder oscillation. In no case, therefore, should the rudder kick be used as a tail-load criterion, since for no airplane is the likelihood of just one rudder cycle at resonance too remote to be considered.

EFFECTS OF NONLINEAR SIDESLIP CHARACTERISTICS

All of the previous results were for cases in which the forces and moments varied linearly with the angle of sideslip. In general, of course, the forces and moments will be nonlinear and some method must be developed to handle such cases. Very often, especially for airplanes with high directional stability, the variations are sufficiently close to the linear that equivalent linear curves may be immediately established by appropriate fairing of the data. In other cases, however, some more adequate means must be supplied such as numerical step-by-step computations, or some analytical method suitable for the problem involved. The methods of nonlinear mechanics developed in references 5 and 6 are particularly adaptable to the problems of this report and their application to such problems is presented in the following material.

Consider first equations (12) and (18). A study of the analogy between these two equations leads to the construction of a third equation similar to equation (16) except that A_1 and B_1 (as defined by equations (20) and (21) are replaced by A and B. Thus the equation

$$\frac{d^2\beta}{d\tau^2} - 2A\frac{d\beta}{d\tau} + \beta B^2 + \frac{2\delta r_o C_{n\delta_r}\mu}{i_c} \sin B\tau = 0 \qquad (43)$$

is the equivalent equation of motion for an airplane whose rudder is applied sinusoidally at resonance and whose ailerons are fixed at zero. The values of A and B, however, must still be determined by the method explained in Appendix A.

The advantage of equation (43) is that it can be readily studied when A and B are not linear. For the study of such nonlinear effects equation (43) is replaced by the equation

$$\frac{d^2\beta}{d\tau^2} + B^2\beta + f\left(\beta, \frac{d\beta}{d\tau}\right) + 2\,\frac{\delta_{r_o} C_{n_{\delta_r}} \mu}{i_c} \sin \alpha\tau = 0 \qquad (44)$$

which is an equation that reduces to equation (43) when the nonlinear terms are neglected. The magnitudes of the parameters in equation (44) are such that its solution will be some periodic function of time. Following the methods of references 5 and 6, it is assumed that the solution is of the form

$$\beta = a \cos (\alpha\tau + \varphi)$$

$$\frac{d\beta}{d\tau} = -a\alpha \sin (\alpha\tau + \varphi) \qquad (45)$$

where a represents the amplitude and $-\frac{\varphi}{\alpha}$ the phase angle of the solution. Both a and φ can be functions of the time but their variation is assumed small and constant over a period.

The nonlinear and forcing terms of equation (44) can now be replaced by the equivalent linear expression

$$\lambda_1 \frac{d\beta}{d\tau} + K_1 \beta$$

so that

$$\lambda_1 \frac{d\beta}{d\tau} + K_1\beta = f\left(\beta, \frac{d\beta}{d\tau}\right) + \frac{2\delta_{r_o} C_{n_{\delta_r}} \mu}{i_c} \sin \alpha\tau \qquad (46)$$

The values of λ_1 and K_1 are determined by balancing the fundamental harmonics between the two sides. Thus if

$$\Phi = \alpha\tau + \varphi$$

$$d\Phi = \alpha\, d\tau \tag{47}$$

then

$$\int_0^{2\pi} (-\lambda_1 a\alpha \sin \Phi + K_1 a \cos \Phi) \sin \Phi d\Phi$$

$$= \int_0^{2\pi} \left[f + \frac{2\mu\delta_{r_o} C_{n\delta_r}}{i_c} \sin (\Phi - \varphi) \right] \sin \Phi d\Phi$$

$$\int_0^{2\pi} (-\lambda_1 a\alpha \sin \Phi + K_1 a \cos \Phi) \cos \Phi d\Phi$$

$$= \int_0^{2\pi} \left[f + \frac{2\mu\delta_{r_o} C_{n\delta_r}}{i_c} \sin (\Phi - \varphi) \right] \cos \Phi d\Phi$$

or, since a and φ are constant over the period,

$$K_1 = \frac{1}{a\pi} \int_0^{2\pi} f(a \cos \Phi, -a\alpha \sin \Phi) \cos \Phi d\Phi - \frac{2\mu\delta_{r_o} C_{n\delta_r}}{a i_c} \sin \varphi \tag{48}$$

$$\lambda_1 = \frac{-1}{a\alpha\pi}\int_0^{2\pi} f(a\cos\Phi, -a\alpha\sin\Phi)\,\Phi d\Phi - \frac{2\mu\delta_{r_o}C_{n_{\delta_r}}}{a\,\alpha\,i_c}\cos\Phi \qquad (49)$$

Now equation (44) can be written

$$\frac{d^2\beta}{d\tau^2} + \lambda_1\frac{d\beta}{d\tau} + (B^2+K_1)\,\beta = 0 \qquad (50)$$

the solution of which will be of the form given in equation (45). Inspection of equation (47) in connection with equation (45) shows that the frequency of the assumed solution will be $d\Phi/d\tau$. But the frequency of a solution to equation (50) will be (neglecting second order terms) $\sqrt{B^2 + K_1}$. Since these two must be equal

$$\frac{d\Phi}{d\tau} = \alpha + \frac{d\varphi}{d\tau} = \sqrt{B^2 + K_1}$$

or

$$\frac{d\varphi}{d\tau} = \sqrt{B^2 + K_1} - \alpha \qquad (51)$$

As for the amplitude, consider equation (50) and let a solution to this equation be $\beta = a\cos\Phi$ where a is a function of the time not necessarily small. Finding the first and second derivatives of this solution and placing them in equation (50) and equating the coefficients of the sine and cosine terms yields the equation

$$-\lambda_1 a \frac{d\Phi}{d\tau} - 2 \frac{da}{d\tau} \frac{d\Phi}{d\tau} = 0$$

or

$$\frac{da}{d\tau} = -\frac{\lambda_1}{2} a \tag{52}$$

Equations (51) and (52) define the period and amplitude of the nonlinear equation (46) within limits of error which will be discussed later. These two equations are especially adaptable when steady-state solutions are desired. In such a case $\frac{da}{d\tau}$ and $\frac{d\Phi}{d\tau}$ are equal to zero so that if the more convenient variables are defined

$$A_e = \frac{1}{2a\pi} \int_0^{2\pi} f(a \cos \Phi, -a\alpha \sin \Phi) \sin \Phi d\Phi \tag{53}$$

and

$$\omega_e^2 = B^2 + \frac{1}{a\pi} \int_0^{2\pi} f(a \cos \Phi, -a\alpha \sin \Phi) \cos \Phi d\Phi \tag{54}$$

Equations (51) and (52) become, respectively,

$$\omega_e^2 = \alpha^2 + \frac{2\mu \delta_{r_o} C_{n\delta_r}}{a i_c} \sin \varphi \tag{55}$$

$$A_e = \frac{2\mu\delta_{r_o} C_{n\delta_r}}{2\,a\,i_c} \cos\varphi \tag{56}$$

Solving these equations for the amplitude, a, gives

$$a = \frac{\left(\frac{2\mu\delta_{r_o} C_{n\delta_r}}{i_c}\right)}{\sqrt{(\alpha^2 - \alpha_e^2)^2 + 4A_e^2}}$$

and for a maximum

$$\alpha = \alpha_e \tag{57}$$

$$a = \frac{1}{2A_e} \frac{2\mu\delta_{r_o} C_{n\delta_r}}{i_c} \tag{58}$$

Consider now the application of equations (57) and (58) to the solution of the motion of an airplane with nonlinear characteristics Let the forces be defined by the equations

$$C_n = \frac{N}{qSb} = M_1\beta + M_2\beta^2 + M_3\beta^3 \tag{59}$$

$$C_Y = \frac{Y}{qS} = l_1\beta + l_2\beta^2 + l_3\beta^3 \tag{60}$$

The value of C_{n_r} due to the tail can be estimated from equation (59) since the angle of attack at the tail caused by the yawing velocity will be rl/V and the yawing moment will be

$$C_n = M_1' \left(\frac{rl}{V}\right) + M_2' \left(\frac{rl}{V}\right)^2 + M_3' \left(\frac{rl}{V}\right)^3$$

or

$$\left(C_{n_r}\right)_{TAIL} = \frac{\partial C_n}{\left(\frac{rb}{2V}\right)} = \frac{2l}{b} M_1' + 2\left(\frac{rb}{2V}\right)\left(\frac{2l}{b}\right)^2 M_2'$$

$$+ 3\left(\frac{rb}{2V}\right)^2 \left(\frac{2l}{b}\right)^3 M_3' \qquad (61)$$

where the prime indicates tail-off minus tail-on values.

The method of including the nonlinear effects into the equivalent equation of motion, equation (44), parallels the development of equation (16) from equation (14). Thus, since the added nonlinear terms are small, equation (44) can be written for the nonlinear forces given by equations (59) and (60) as

$$\frac{d^2\beta}{d\tau^2} - 2A \frac{d\beta}{d\tau} + B^2\beta + \frac{2\mu\delta_{r_o} C_{n\delta_r}}{i_c} \sin \alpha\tau - l_2\beta \frac{d\beta}{d\tau}$$

$$\frac{3}{2} l_3\beta^2 \frac{d\beta}{d\tau} - \left(\frac{2l}{b}\right)^2 \frac{1}{2\mu i_c}\left[\frac{3\left(\frac{2l}{b}\right)}{2\mu}\left(\frac{d\beta}{d\tau}\right)^3 M_3' - 2\left(\frac{d\beta}{d\tau}\right)^2 M_2'\right]$$

$$+ \beta^2 M_2 \frac{2\mu}{i_c} + \beta^3 M_3 \frac{2\mu}{i_c} = 0 \qquad (62)$$

where only the variations of forces and moments with sideslip have been considered.

Now using equations (53) and (54)

$$A_\beta = \left[-A - \left(\frac{3}{16} l_\beta + \frac{9}{8} \frac{\left(\frac{2l}{b}\right)^2 N_\beta' c^2}{4 \mu^2 i_B} \right) a^2 \right] \alpha \qquad (63)$$

$$a_0^2 = B^2 + \frac{3}{4} a^2 \frac{2\mu}{i_C} N_\beta \qquad (64)$$

and if the variables s_1 and s_2 are defined so that

$$s_1 = \frac{1}{A} \left[\frac{3}{16} l_\beta + \frac{9}{16} \left(\frac{2l}{b} \right)^2 \frac{B^2}{4\mu^2 i_C} N_\beta' \right] \qquad (65)$$

and

$$s_2 = \frac{3}{2} \frac{\mu}{i_C} \frac{M^3}{B^2} \qquad (66)$$

and the conditions for a maximum amplitude presented in equations (57) and (58) are used, there results

$$\beta^8 s_1^2 s_2 + \beta^6 (2s_1 s_2 + s_1^2) + \beta^4 (s_2 + 2s_1) + \beta^2 - \beta_{A_R}^2 = 0 \quad (67)$$

where β is the maximum sideslip developed with the nonlinear characteristics and β_{A_R} is the sideslip if the nonlinear terms are zero. Equation (67) is a quartic in β^2 and its solution may be found quickly by numerical methods since only one root is required and this root must be real and somewhat less than β_{A_R}.

It should be noticed that the terms containing l_2, M_2, and M_2' do not appear in equations (63) and (64) and, therefore, do not affect the final amplitude or period. Such results can be generalized to any value of l_k, M_k and M_k' where k is even. Physically this has the meaning that the lack of symmetry about the $\beta = 0$ axis does not affect the steady-state amplitude and period of the airplane motion. Thus the first step in replacing an experimental curve by a power series is to average the positive and negative sides, that is set $f(\beta) = \frac{1}{2}[f(\beta) - f(-\beta)]$. If the resulting curve has a curvature proportional to β^k where k is even, let $\beta^k = |\beta|\beta^{k-1}$ and use this in equations (53) and (54)

In order to obtain some idea of the effects of nonlinearity on the maximum angles of sideslip in a fishtailing maneuver, the curves shown in figures 13 and 14 were chosen as possible variations of C_Y and C_n with β. The curves show both the nonlinear variations used, the equations of which are

$$\begin{aligned} C_n &= 0.024\beta + 0.2\beta^3 \\ C_Y &= -0.4\beta - 0.8\beta^3 \end{aligned} \quad (68)$$

and also some experimental data taken from tests on a fighter airplane. The experimental data were included to show that the choices were not unreasonable.

Figure 15 presents the results of using equation (68) together with the derivatives as given for configurations 5 and 6 in evaluating the maximum sideslip in a fishtailing maneuver. The figure shows the maximum value of $\beta^\circ_{\text{Nonlinear}}$ for the nonlinear configuration plotted against the value $\beta^\circ_{A_R}$, the maximum sideslip resulting if the nonlinear terms are neglected. The resulting reduction in sideslip angle is, of course, a function of the amplitude, but it is seen that when the linear theory predicts 30° of sideslip, the nonlinear theory predicts around 20°, a reduction of 10° in maximum sideslip.

The effects of the nonlinear terms in the transient stage can also be found from equations (51) and (52) but such results would be somewhat less reliable, since the theory averages the nonlinear terms over a period, a procedure which would introduce more error when the amplitude of succeeding cycles was varying significantly. However, the results of the linear theory are deemed sufficient inasmuch as figure 10 can be used with the linear value of the ratio A/B, provided that the value of β_{A_R} in the ratio β_{A_N}/β_{A_R} is replaced by the value derived on the basis of the nonlinear theory.

Some idea of the error involved in the nonlinear theory presented in this report can be obtained by a study of the special case of neutral dynamic stability with a linear and cubic variation of C_n with β. In such a case the equation of motion becomes

$$\frac{d^2\beta}{d\tau^2} + B^2\beta + \beta^3 M_3 \frac{2\mu}{i_c} = 0 \tag{69}$$

Equation (69) has the advantage that an exact solution can be found for it and this solution can be compared with that found by the methods of references 5 and 6 which is given by equation (67) with $s_1 = 0$.

To solve equation (69) let

$$\frac{d\beta_t}{d\tau} = \beta_2; \quad \beta_t = \beta$$

then

$$\frac{d\beta_2}{d\beta_t} = \frac{-B^2\beta_t - M_s \frac{2\mu}{i_c} \beta_t^3}{\beta_2}$$

or

$$\frac{1}{2} \beta_2^2 = -B^2 \frac{1}{2} \beta_t^2 - (1/4) M_s \frac{2\mu}{i_c} \beta_t^4 + \text{Constant} \tag{70}$$

Now when $\beta_2 = 0$, β_t is a maximum so that

$$0 = -B^2 (1/2) \beta_{t_o}^2 - (1/4) M_s \frac{2\mu}{i_c} \beta_{t_o}^4 + \text{Constant}$$

and when

$$M_s = 0, \quad \beta_{t_o} = \beta_{AR}$$

where β_{AR} is the maximum sideslip derived from the linear theory.

Hence

$$\frac{\mu}{i_c} \frac{M^3}{B^2} \beta_{t_o}^4 + \beta_{t_o}^2 - \beta_{AR}^2 = 0$$

or by using s_2 as defined in equation (66)

$$\beta_{t_o} = \sqrt{\frac{-3 + \sqrt{9 + 24 s_2 \beta_{AR}^2}}{4 s_2}}$$

So the ratio of the approximate value of β_{a_o} given by equation (67) with $s_1 = 0$, to the maximum sideslip rigorously derived, β_{t_o}, is

$$\frac{\beta_{a_o}}{\beta_{t_o}} = \sqrt{\frac{-2 + 2\sqrt{1 + 4 s_2 \beta_{AR}^2}}{-3 + \sqrt{9 + 24 s_2 \beta_{AR}^2}}} \qquad (71)$$

This ratio is plotted in figure 16 as a function of β_{A_R} for various values of s_2. The error of the results presented in figure 15 as determined from figure 16 would be around 5 to 6 percent at a β_{A_R} of 30°. This amounts to an increase of about 1° of sideslip in 20° of sideslip for the nonlinear results. These results correspond

to a cubic variation (which represents a fairly large departure from linearity) of C_n with β for the case of neutral stability as given by equation (69). This comparison is therefore believed to provide an adequate check of the general equation (equation (67)).

CONCLUSIONS

A general theory is developed for rudder oscillating maneuvers in which various amounts of aileron deflection are applied. On the basis of this theory which was verified by the specific analysis of 27 representative airplane configurations, the following general conclusions are drawn:

1. Of the rudder-oscillating maneuvers considered, the aileron-fixed maneuver appears to be the most useful as a criterion for vertical-tail loads. Although sideslip angles as much as 18 percent greater can be obtained by particularly adverse combinations of rudder and aileron control motions, the probability of maintaining such adverse combinations over a sufficient time interval is considered remote.

2. The rudder-oscillating, aileron-fixed maneuver produces vertical-tail loads which compare with those produced in other dynamic maneuvers as follows:

   (a) The fishtailing maneuver can, for certain airplane configurations, be more critical in producing tail loads than the rolling pull-out maneuver.

   (b) For certain airplane configurations one and one-half cycles of rudder motion are sufficient to produce tail loads of the same order of magnitude as those produced by rolling pull-out maneuvers.

   (c) For all airplane configurations one cycle of rudder motion is sufficient to produce more sideslip than that obtained from the rudder-kick maneuver.

3. Methods are developed for including the effect on the motion of the airplane of nonlinear variations of forces and moments with angle of sideslip.

Ames Aeronautical Laboratory,
National Advisory Committee for Aeronautics,
Moffett Field, Calif.

APPENDIX A

The values of A and B used in the formulas in this report can only be determined by finding the complex roots to the quartic given in terms of S by the equation

$$\begin{vmatrix} \left(s - \frac{C_{l_p}}{i_a}\right) & -\left(\frac{C_{l_r}}{i_a}\right) & \left(-C_{l_\beta}\ \frac{2\mu}{i_a}\right) \\ \left(-\frac{C_{n_p}}{i_c}\right) & \left(s - \frac{C_{n_r}}{i_c}\right) & \left(-C_{n_\beta}\ \frac{2\mu}{i_c}\right) \\ \left(-\frac{1}{2}\frac{C_L}{s}\right) & (1) & \left(s - \frac{1}{2}C_{Y_\beta}\right) \end{vmatrix} = 0 \qquad (A1)$$

The values of the derivatives are usually such that equation (A1) will have two real and two complex roots. In such cases the value of A is equal to the real part and the value of B is equal to the imaginary part of either one of the complex roots. In cases where A is zero or positive, equations such as equation (12) do not apply because the motion is divergent and no steady-state solutions exist. Such cases do have meaning in figure 12, however,

where they represent the line $A/B = 0$.

The values of A and B obtained for the configurations of table I are listed in table III and interpolation can be made in this table to many airplane designs.

REFERENCES

1. Jones, Robert T.: A Simplified Application of the Method of Operators to the Calculation of Disturbed Motions of an Airplane. NACA Rep. No. 560, 1936.

2. Churchill, Ruel V., Modern Operational Mathematics in Engineering. McGraw-Hill Book Co., Inc., New York, 1944.

3. Boshar, John, and Davis, Philip: Consideration of Dynamic Loads on the Vertical Tail by the Theory of Flat Yawing Maneuvers. NACA TN No. 1065, 1946.

4. White, Maurice, D., Lomax, Harvard; and Turner, Howard L.: Sideslip Angles and Vertical-Tail Loads in Rolling Pull-out Maneuvers. NACA TN No. 1122, 1947.

5. Kryloff, N. and Bogoliuboff, N.: Introduction to Nonlinear Mechanics. Princeton University Press, 1943.

6. Minorsky, N.: Introduction to Nonlinear Mechanics. Parts I to IV. The David W. Taylor Model Basin, United States Navy, 1945.

TABLE I.- COMBINATIONS OF AIRPLANE STABILITY PARAMETERS USED IN NUMERICAL COMPUTATIONS

Configuration	C_{n_β}	C_{l_β}	C_{Y_β}	C_{l_r}	C_{l_p}	C_{n_p}	C_{n_r}	i_a	i_c	μ	C_L	Principal variable
1	0.096	-0.12	-0.4	0.06	-0.42	-0.03	-0.120	0.12	0.18	10	0.2	
2	.096	0	-.4	.06	-.42	-.03	-.120	.12	.18	10	.2	—
3	.048	-.12	-.4	.06	-.42	-.03	-.072	.12	.18	10	.2	
4	.048	0	-.4	.06	-.42	-.03	-.072	.12	.18	10	.2	Basic
5	.024	-.12	-.4	.06	-.42	-.03	-.048	.12	.18	10	.2	
6	.024	0	-.4	.06	-.42	-.03	-.048	.12	.18	10	.2	
7	.024	0	-.4	.06	-.42	-.03	-.048	.06	.18	10	.2	
8	.024	0	-.4	.06	-.42	-.03	-.048	.12	.12	10	.2	
9	.024	-.12	-.4	.06	-.42	-.03	-.048	.06	.18	10	.2	
10	.024	-.12	-.4	.06	-.42	-.03	-.048	.12	.12	10	.2	i_a and i_c
11	.096	-.12	-.4	.06	-.42	-.03	-.120	.06	.18	10	.2	
12	.096	-.12	-.4	.06	-.42	-.03	-.120	.12	.12	10	.2	
13	.024	0	-.4	.06	-.42	-.03	-.048	.12	.18	2.5	.2	
14	.024	0	-.4	.06	-.42	-.03	-.048	.12	.18	40	.2	
15	.096	0	-.4	.06	-.42	-.03	-.120	.12	.18	2.5	.2	
16	.096	0	-.4	.06	-.42	-.03	-.120	.12	.18	40	.2	μ
17	.096	-.12	-.4	.06	-.42	-.03	-.120	.12	.18	2.5	.2	
18	.096	-.12	-.4	.06	-.42	-.03	-.120	.12	.18	40	.2	
19	.024	0	-.4	.06	-.42	-.03	-.100	.12	.18	10	.2	
20	.024	-.12	-.4	.06	-.42	-.03	-.100	.12	.18	10	.2	
21	.024	0	-.8	.06	-.42	-.03	-.048	.12	.18	10	.2	C_{Y_β}
22	.024	-.12	-.8	.06	-.42	-.03	-.048	.12	.18	10	.2	and
23	.096	-.12	-.4	.06	-.42	-.03	-.172	.12	.18	10	.2	C_{n_r}
24	.096	-.12	-.8	.06	-.42	-.03	-.120	.12	.18	10	.2	
25	.024	0	-.4	.03	-.42	-.015	-.047	.12	.18	10	.1	
26	.024	-.12	-.4	.03	-.42	-.015	-.047	.12	.18	10	.1	C_L
27	.096	-.12	-.4	.03	-.42	-.015	-.119	.12	.18	10	.1	

TABLE II.- LIST OF COEFFICIENTS, FREQUENCIES, AND EXPONENTIALS FOR EQUATION (2) FOR THE CONFIGURATIONS LISTED IN TABLE I

Configuration	λ_1	λ_2	A	B	C_1	C_2	C_3	C_4
1	-0.01865	-3.725	-0.3115	3.379	0027	0092	-0119	-0.2869
2	.01403	-3.494	-.4434	3.269	0000	-0010	0009	-.3069
3	-.02210	-3.781	-.1486	2.522	0053	0138	-0191	-.3770
4	.01398	-3.487	-.3134	2.317	0000	-0018	0017	-.4340
5	-.02711	-3.818	-.0610	1.965	0098	0171	-0269	-.4764
6	.01389	-3.482	-.2492	1.641	0001	-0024	0024	-.6140
7	.01392	-6.977	-.2516	1.628	0001	-0008	-0006	-.6137
8	.01390	-3.475	-.3194	2.010	0001	-0028	0028	-.5019
9	-.02705	-7.184	-.1277	2.025	0098	0032	-0130	-.4833
10	-.02840	-3.880	-.0958	2.332	0071	0187	-0258	-.3986
11	-.01861	-7.166	-.3411	3.447	0027	0026	-0053	-.2851
12	-.01895	-3.743	-.4693	4.087	0018	0084	-0103	-.2381
13	.01298	-3.476	-.2516	.822	0017	-0035	0021	-1.2305
14	.01414	-3.494	-.2433	3.276	0000	-0009	0010	-.3064
15	.01347	-3.480	-.4500	1.625	0003	-0029	0026	-.6310
16	.01418	-3.506	-.4372	6.536	0000	-0002	0003	-.1524
17	-.01811	-3.480	-.3845	1.714	0106	-0028	-0079	-.5907
18	-.01879	-3.871	-.2383	6.628	0007	0063	-0068	-.1474
19	.01359	-3.481	-.3942	1.632	0002	-0027	0025	-.6179
20	-.06640	-3.828	-.1804	1.953	0193	0187	-0381	-.4782
21	.01359	-3.483	-.3489	1.642	0002	-0025	0023	-.6140
22	-.02678	-3.832	-.1541	1.968	0097	0185	-0281	-.4742
23	-.03213	-3.728	-.4475	3.361	0038	0098	-0136	-.2884
24	-.01848	-3.732	-.4082	3.384	0027	0098	-0124	-.2863
25	.00350	-3.500	-.2345	1.625	0000	-0003	0006	-.6129
26	-.01881	-3.674	-.1340	1.810	0065	0108	-0173	-.5316
27	-.01310	-3.618	-.3651	3.317	0015	0053	0069	-.2964

TABLE III.- LIST OF IMPORTANT PARAMETERS USED IN THE REPORT FOR THE CONFIGURATIONS LISTED IN TABLE I.

Configuration	l/B	H_1	H_2	A/B
1	0.2959	-0.0123	-0.0125	-0.092
2	.3059	-.0092	-.0095	-.136
3	.3965	-.0434	-.0319	-.059
4	.4316	-.0246	-.0176	-.135
5	.5089	-.1557	-.0888	-.031
6	.6094	-.0522	-.0260	-.152
7	.6105	-.0301	-.0077	-.154
8	.4975	-.0366	-.0175	-.159
9	.4938	-.0453	-.0141	-.063
10	.4288	-.0924	-.0503	-.041
11	.2901	-.0086	-.0047	-.099
12	.2447	-.0065	-.0066	-.115
13	1.2165	-.1199	-.0033	-.306
14	.3053	-.0173	-.0168	-.174
15	.6154	-.0286	-.0167	-.277
16	.1530	-.0020	-.0039	-.067
17	.5834	-.0311	-.0189	-.224
18	.1595	-.0036	-.0066	-.036
19	.6127	-.0327	-.0183	-.242
20	.5120	-.0523	-.0318	-.093
21	.6090	-.0377	-.0174	-.212
22	.5081	-.0618	-.0335	-.129
23	.2974	-.0087	-.0089	-.133
24	.2955	-.0096	-.0094	-.120
25	.6116	-.0279	-.0137	-.144
26	.5525	-.0408	-.0218	-.074
27	.3015	-.0055	-.0055	-.110

TABLE IV.- RATIO OF THE SIDESLIP ANGLES DEVELOPED IN VARIOUS MANEUVERS

Configuration	$\frac{\beta_{A_R True}}{\beta_{A_R Approx.}}$	$\frac{\beta_{B_R}}{\beta_{A_R}}$
1	1.006	0.747
2	1.000	1.025
3	.954	.541
4	1.003	1.048
5	.945	.316
6	1.004	1.076
7	1.001	1.084
8	1.007	1.070
9	.985	.682
10	.931	.372
11	.984	.833
12	.977	.799
13	1.000	1.089
14	.989	1.049
15	1.022	1.035
16	.995	1.011
17	1.009	.933
18	.977	.559
19	1.000	1.046
20	.942	.573
21	1.002	1.055
22	.936	.558
23	.976	.800
24	.973	.795
25	1.000	1.021
26	.967	.648
27	1.010	.864

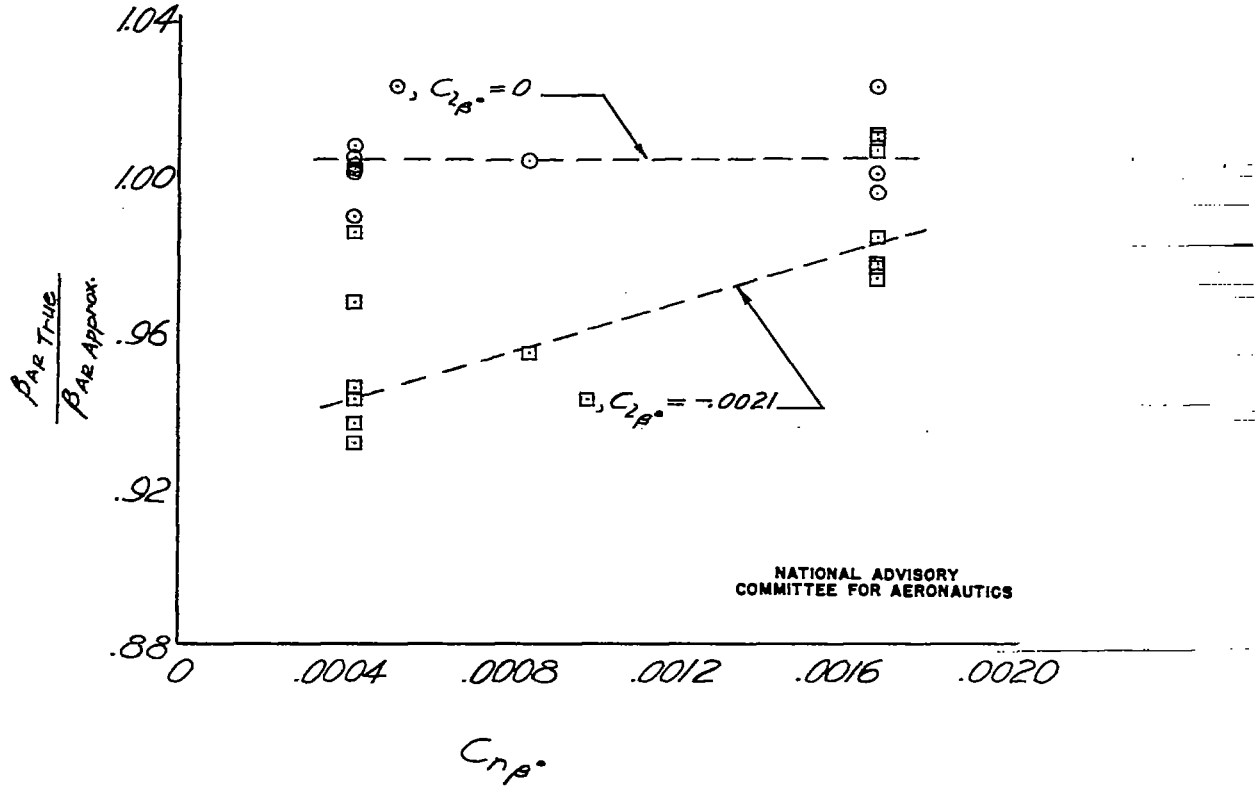

Figure 1 – Comparison between the maximum angles of sideslip computed from equation 12 and from equation 2 with no approximations. Maneuver A.

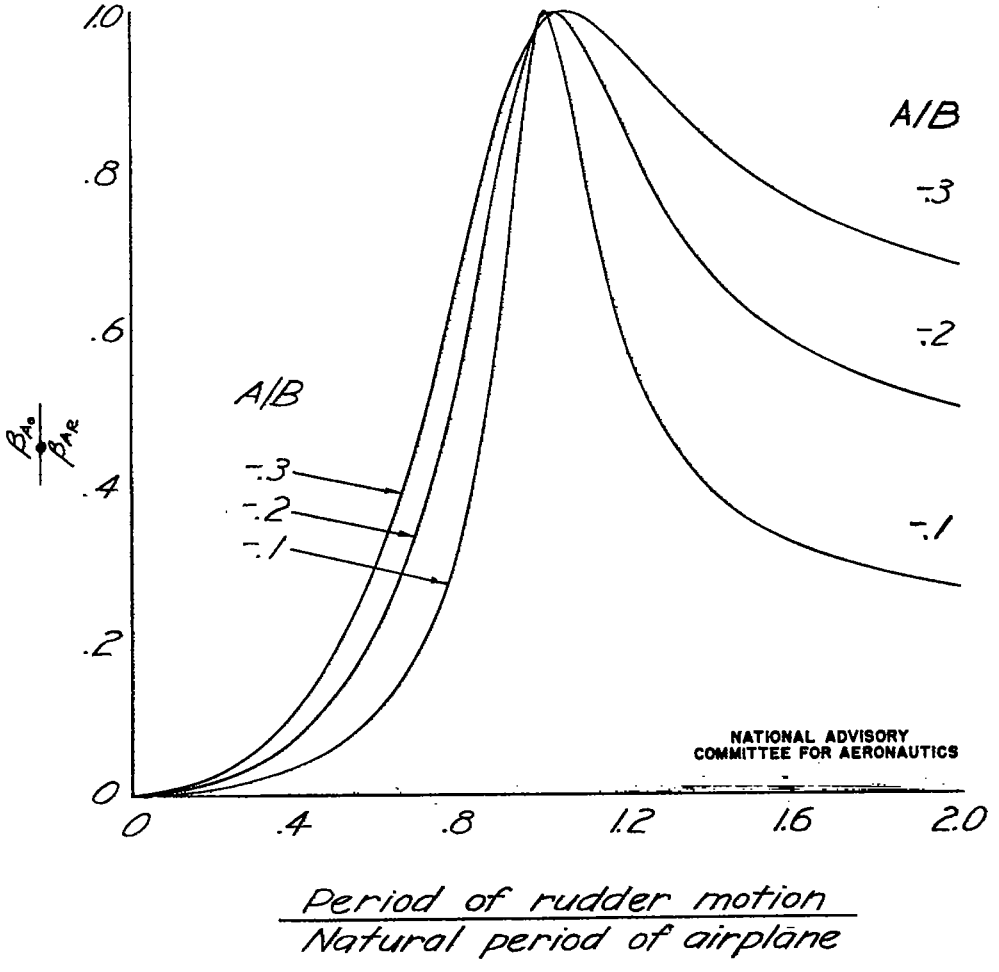

Figure 2 Ratio of the maximum angle of sideslip to the maximum resonant angle of sideslip for various values of A/B. Maneuver A.

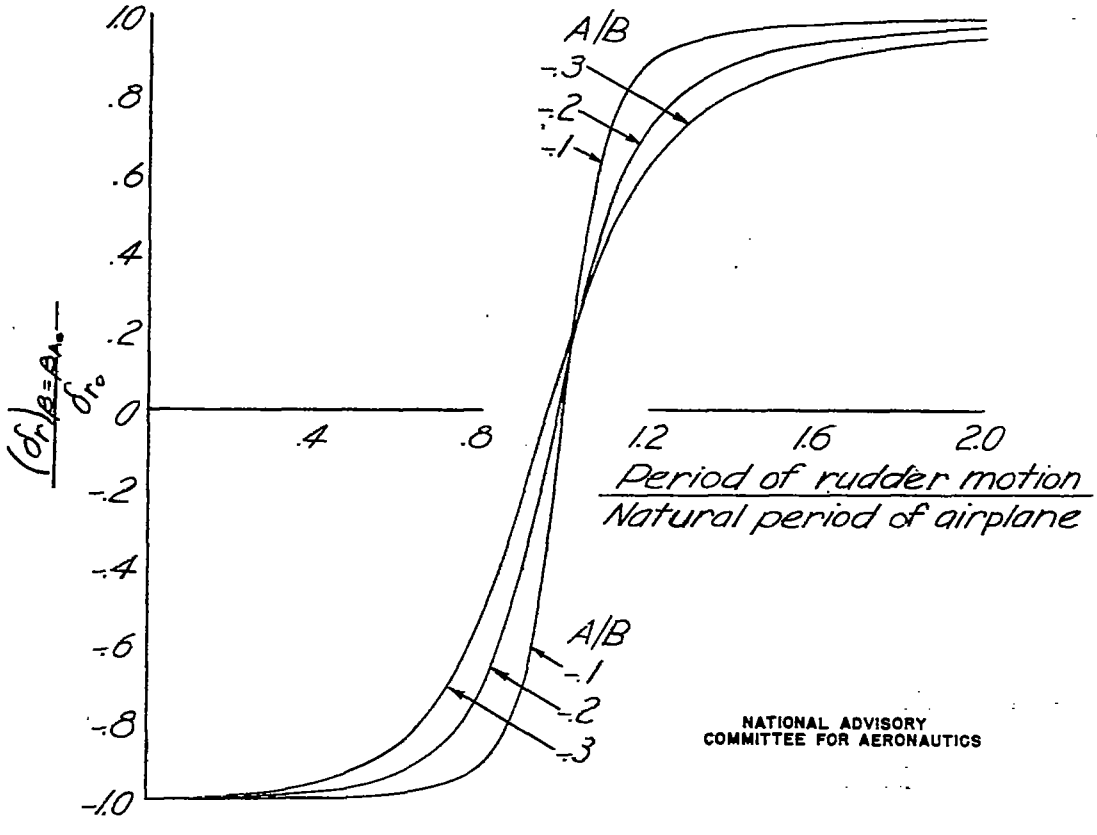

Figure 3 – Ratio of the rudder angle at maximum sideslip to the maximum rudder angle for various values of A/B. Maneuver A.

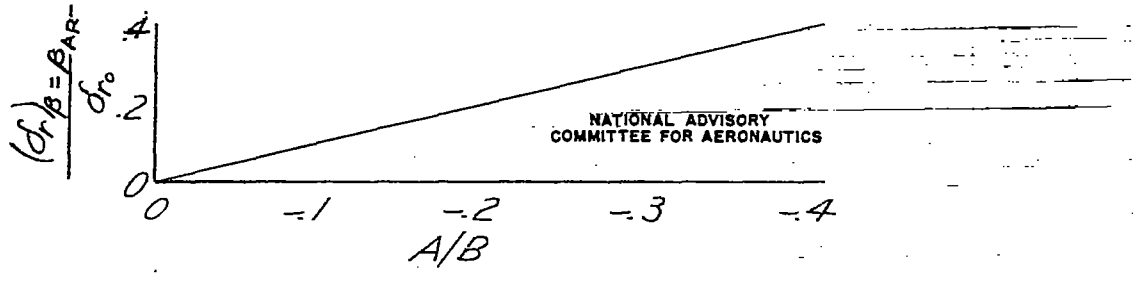

Figure 4 – Ratio of the rudder angle at the maximum resonant value of sideslip to the maximum rudder angle for values of A/B. Maneuver A.

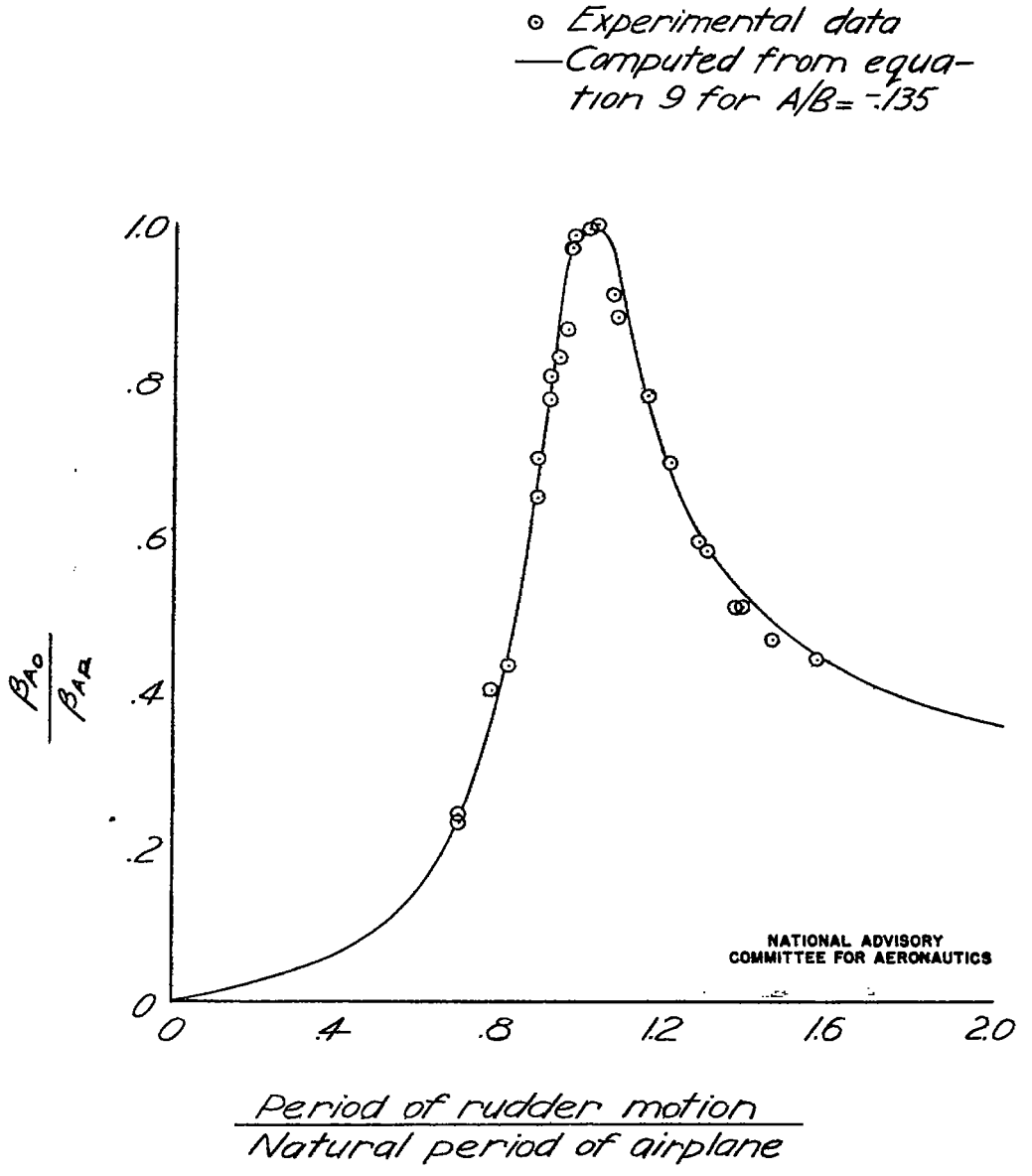

Figure 5 – Comparison of the ratio of maximum angle of sideslip to the maximum resonant angle of sideslip as determined from theory and flight test data. Maneuver A.

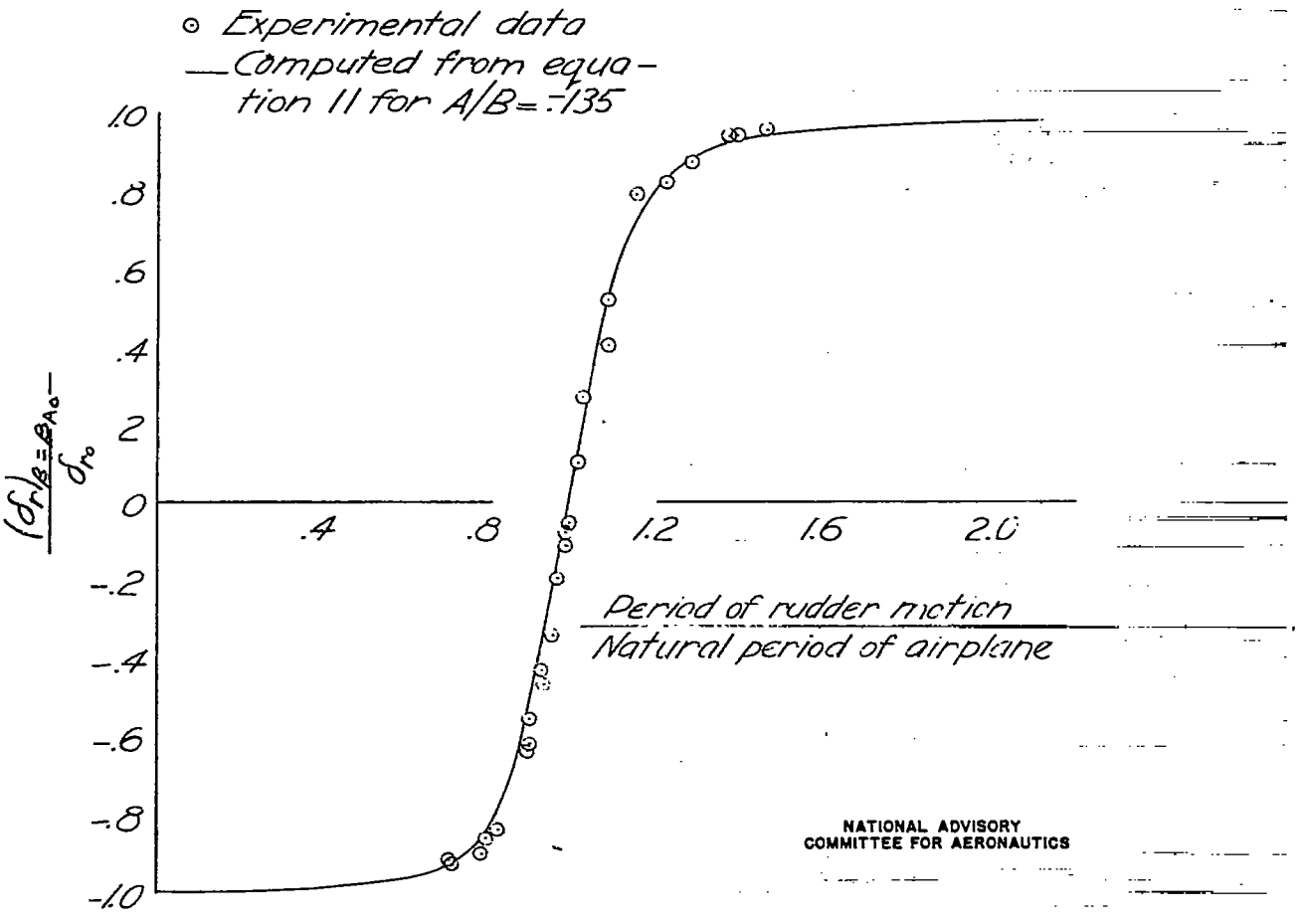

Figure 6 - Comparison of the ratio of the rudder angle at maximum sideslip to the maximum rudder angle as determined from theory and flight test data. Maneuver A.

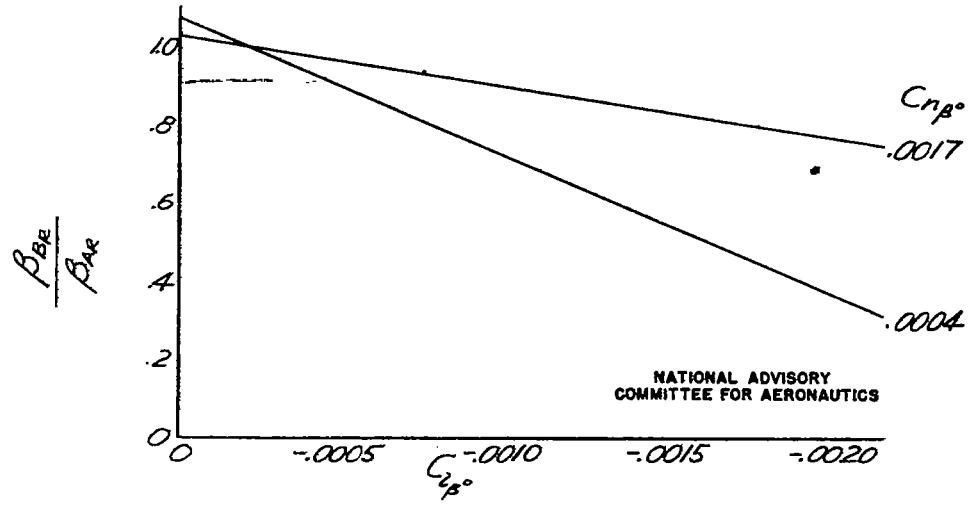

Figure 7 – Ratio of the maximum resonant sideslip developed in a maneuver with wings level to that developed in a maneuver with ailerons locked for various values of $C_{l_{\beta^\circ}}$ and $C_{n_{\beta^\circ}}$.

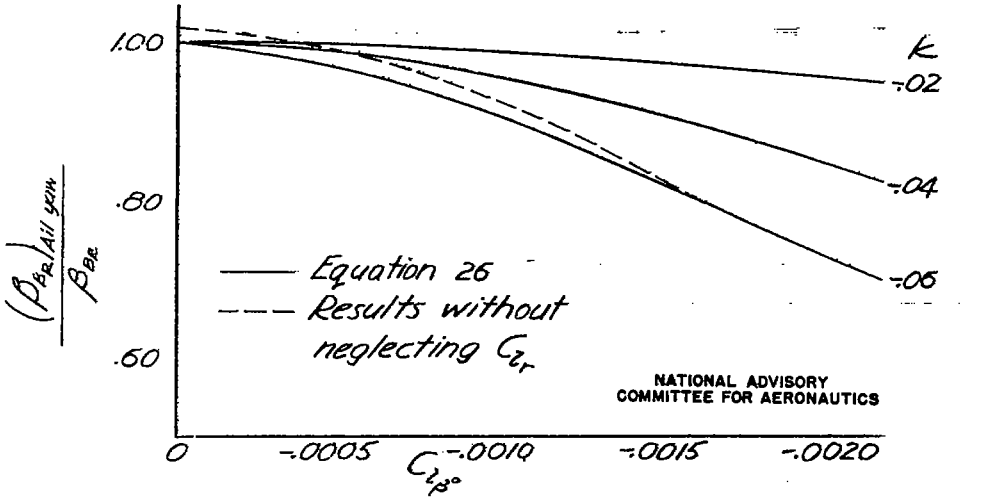

Figure 8 – Ratio of the maximum resonant angle of sideslip developed considering aileron yaw to that neglecting aileron yaw for various values of $C_{l_{\beta^\circ}}$ and k. For $\mu = 10$, $i_c = .18$, $C_{Y_\beta} = -.4$, $C_{n_r} = -.048$, $C_{n_{\beta^\circ}} = .0004$.

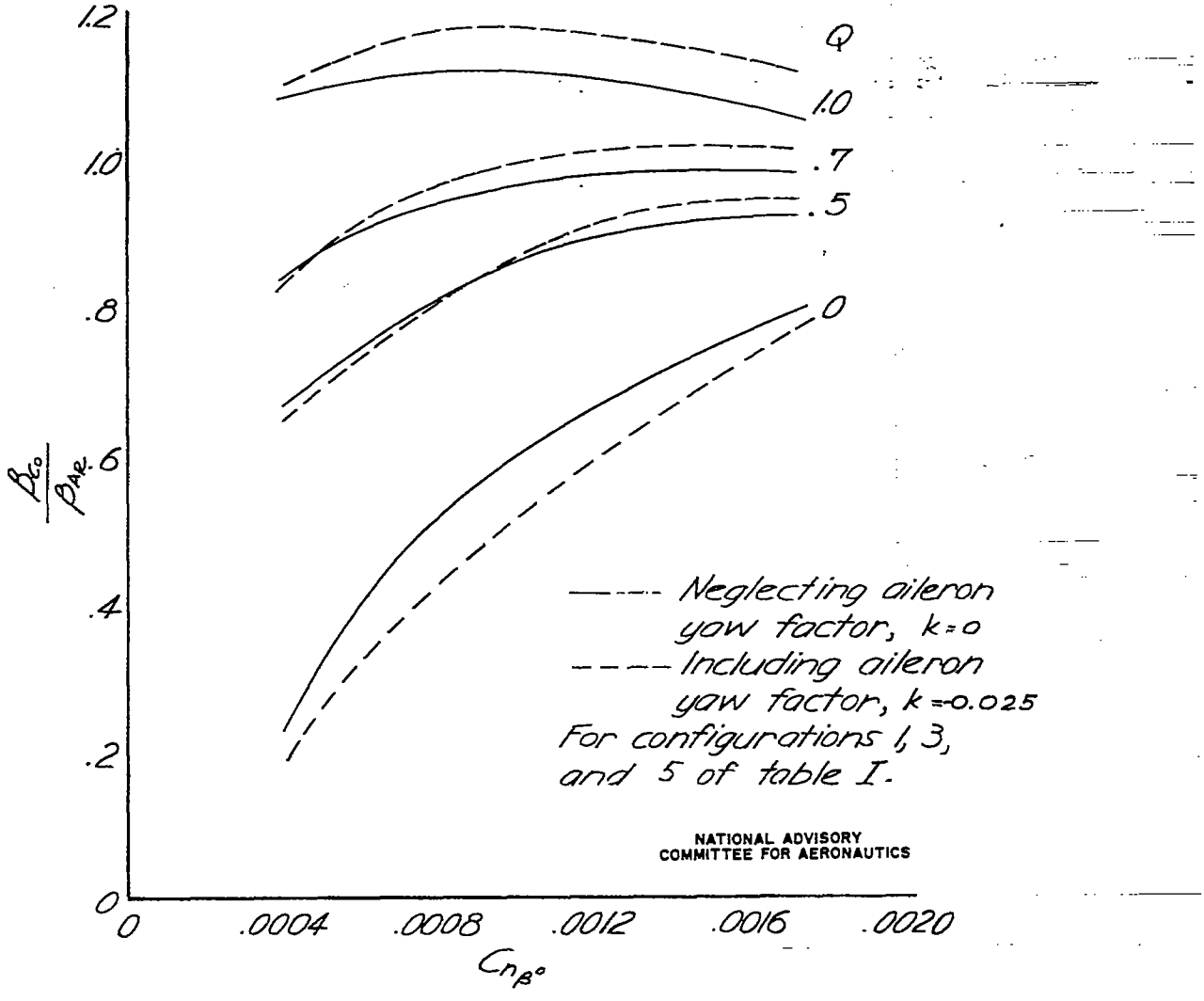

Figure 9 – Ratio of the maximum sideslip in a maneuver in which the roll is reduced (1-Q)100 percent by the ailerons to that in a maneuver in which the ailerons are fixed for various values of C_{n_β}, Q and k.

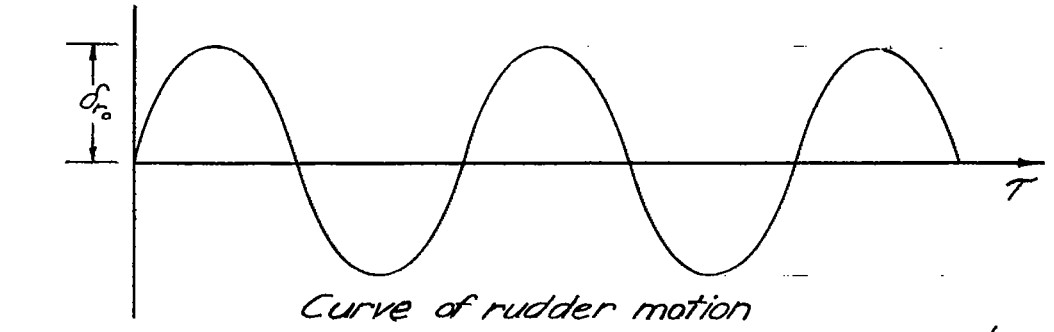

Curve of rudder motion

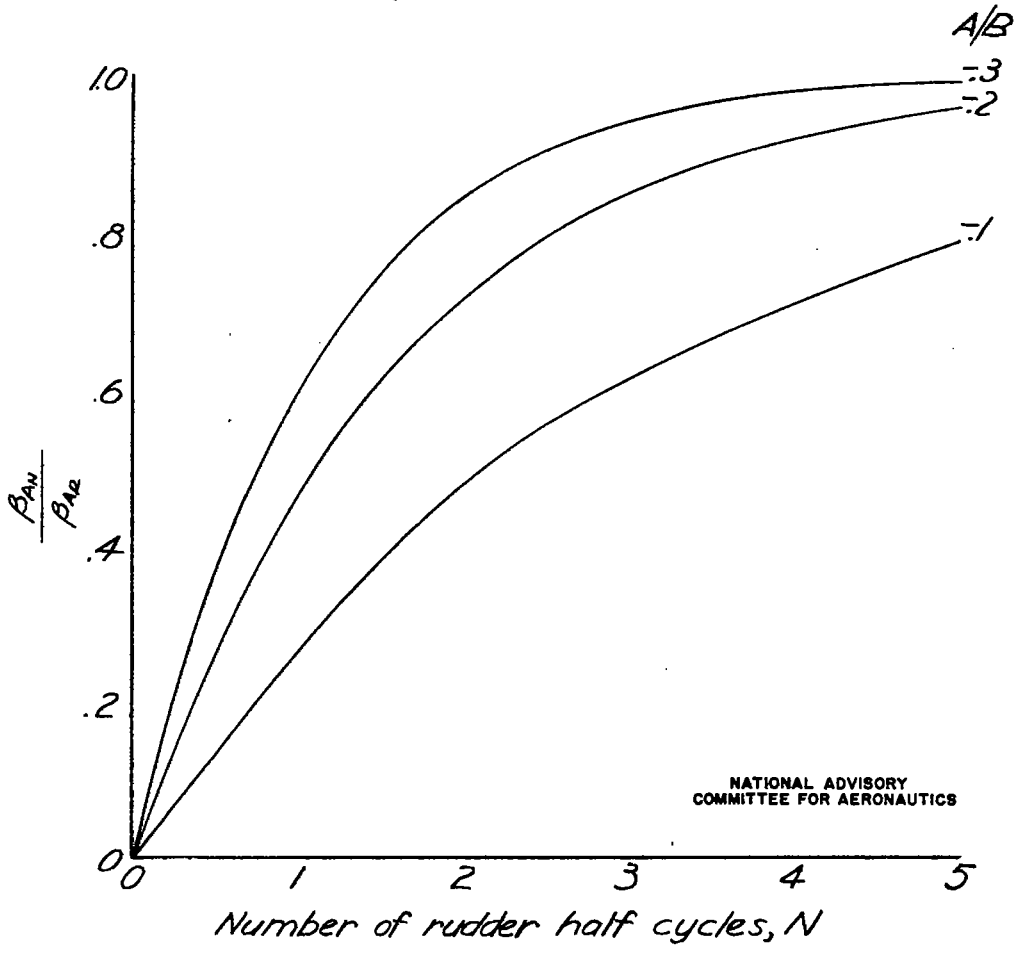

Number of rudder half cycles, N

Figure 10 – Ratio of the maximum resonant value of sideslip at the end of N/2 cycles to that at steady state for various values of N and A/B.

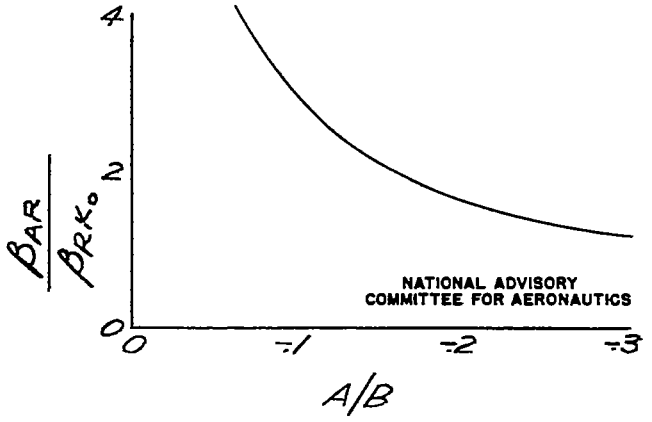

Figure 11 – Ratio of the maximum resonant sideslip angle from a fishtail maneuver to the maximum sideslip angle from a rudder kick maneuver for various values of A/B.

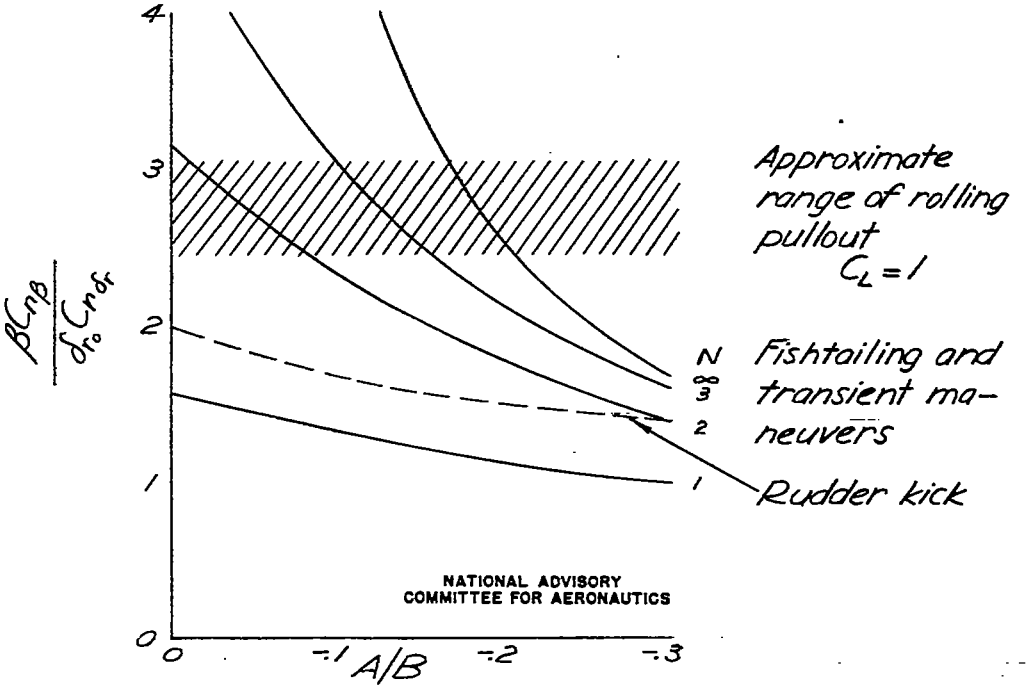

Figure 12 – Comparison of the maximum sideslip angles developed in various dynamic maneuvers.

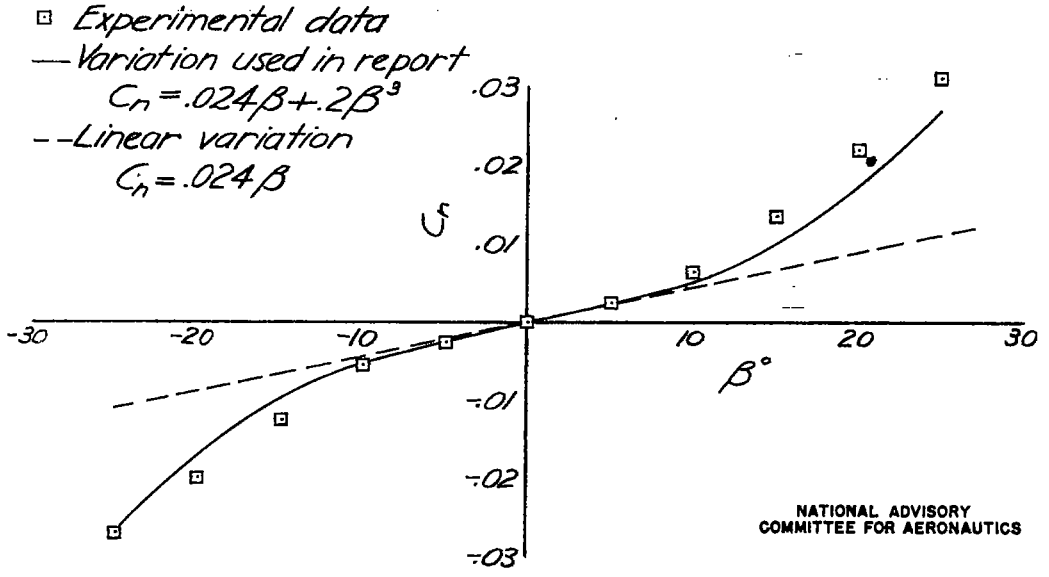

Figure 13 – Variation of yawing moment coefficient with angle of sideslip.

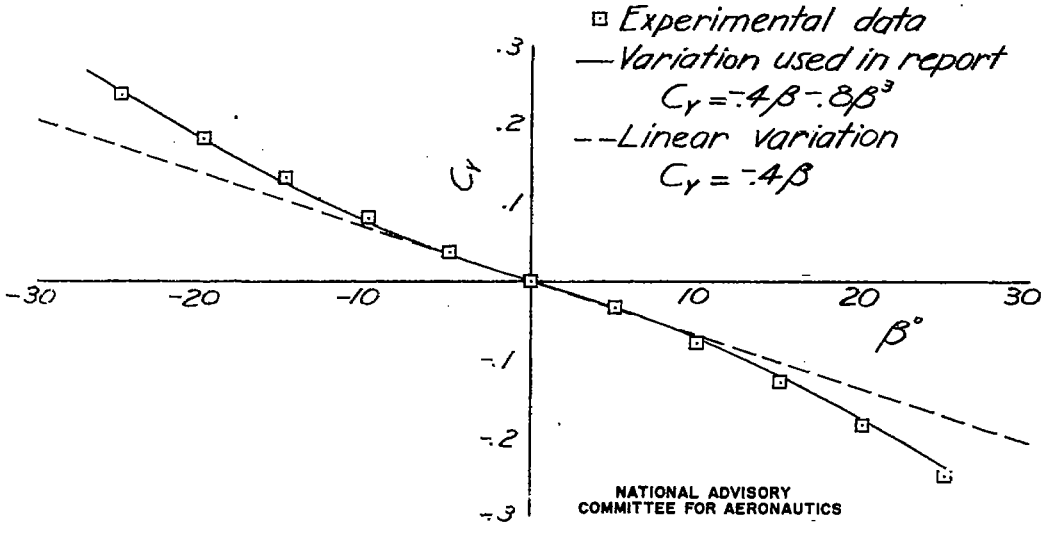

Figure 14 – Variation of lateral force coefficient with angle of sideslip.

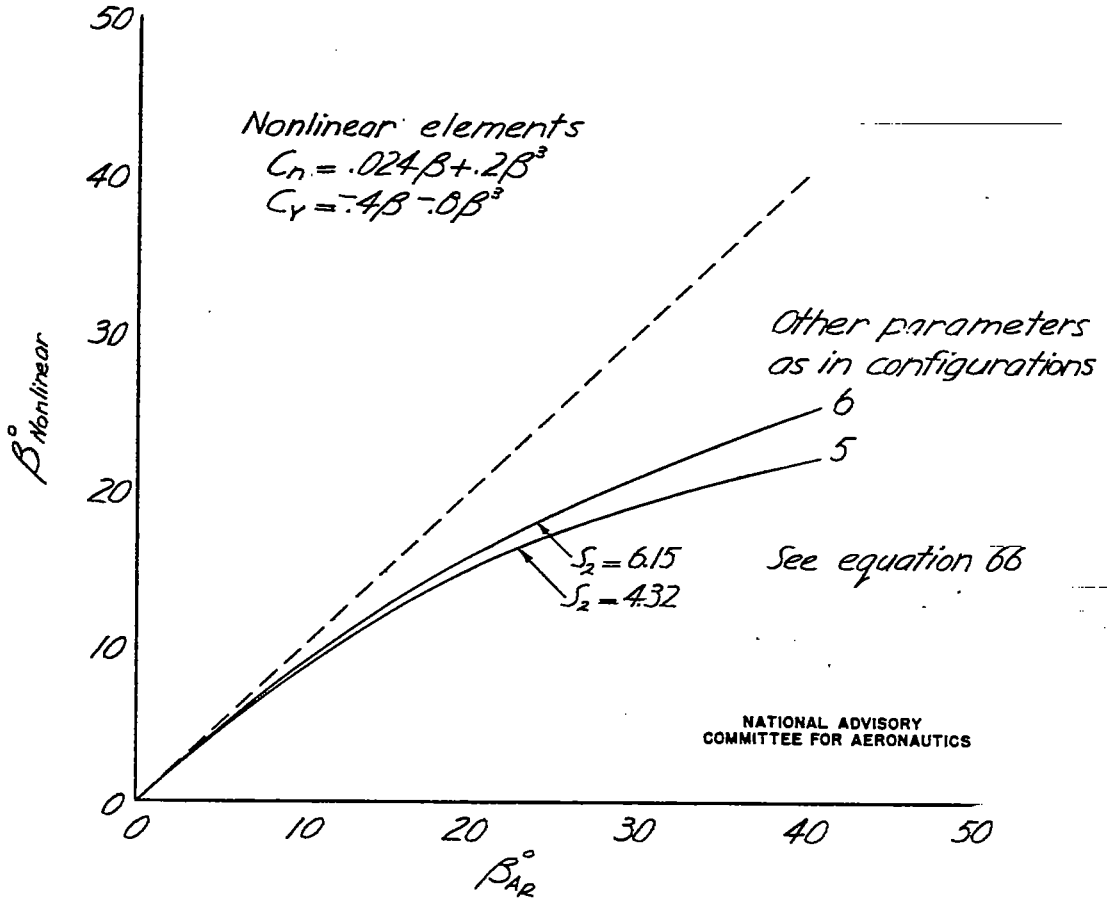

Figure 15 — Comparison of the angle of sideslip derived including nonlinear terms with that neglecting nonlinear terms. Maneuver A.

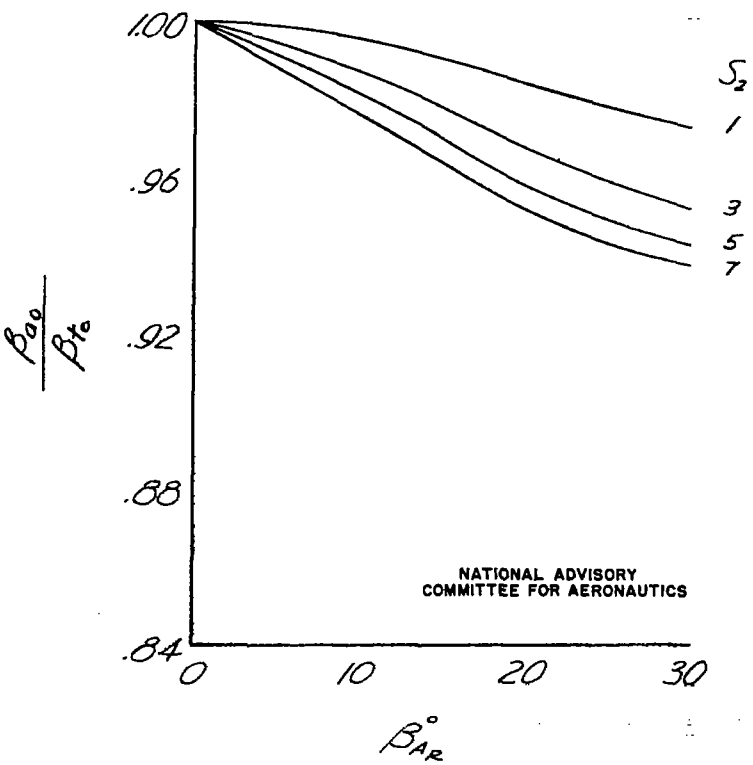

Figure 16 – Comparison of the maximum resonant value of sideslip developed from the approximate nonlinear theory of this report with that developed from rigorous theory for the special case of neutral stability.